Basin-scale impacts of hydropower development on the Mompós Depression wetlands, Colombia

Héctor Angarita[1,2], Albertus J. Wickel[3], Jack Sieber[3], John Chavarro[4], Javier A. Maldonado-Ocampo[5], Guido A. Herrera-R[5], Juliana Delgado[2], David Purkey[3]

[1] Grupo de ecología y territorio, Pontificia Universidad Javeriana. Bogotá, Colombia
[2] The Nature Conservancy
[3] Stockholm Environment Institute US Center
[4] Centro de Investigación en Ciencias y Recursos GeoAgroAmbientales CENIGAA
[5] Laboratorio de Ictiología, Unidad de Ecología y Sistemática (UNESIS), Departamento de Biología, Facultad de Ciencias, Pontificia Universidad Javeriana. Bogotá, Colombia

Correspondence to: H. Angarita (hangarita@javeriana.edu.co)

Abstract: A number of large hydropower dams are currently under development or in an advanced stage of planning in the Magdalena River basin, Colombia, spelling uncertainty for the Mompós Depression wetlands, one of the largest wetland systems in South America at 3400 km^2. Annual large-scale inundation of floodplains and associated wetlands regulates water-, nutrient-, and sediment cycles, which in turn sustain a wealth of ecological processes and ecosystem services, including critical food supplies. In this study, we implemented an integrated approach focused on key attributes of ecologically functional floodplains: (1) hydrologic connectivity between the river and the floodplain, and between upstream and downstream sections; (2) hydrologic variability patterns and their links to local and regional processes; and (3) the spatial scale required to sustain floodplain-associated processes and benefits, like migratory fish biodiversity. The implemented framework provides an explicit quantification of the non-linear or direct response relationship of those considerations to hydropower development. The proposed framework was used to develop a comparative analysis of the potential effects of hydropower expansion to meet projected electricity requirements by 2050. As part of this study, we developed an enhancement of the Water Evaluation and Planning system (WEAP) that allows resolution of the floodplains water balance at a medium scale (~1000 to 10 000 km^2) and evaluation of the potential impacts of upstream water management practices. In the case of the Mompós Depression wetlands, our results indicate that potential additional impacts of new hydropower infrastructure with respect to baseline conditions can range up to one order of magnitude between scenarios that are comparable in terms of energy capacity. Fragmentation of connectivity corridors between lowland floodplains and upstream spawning habitats and reduction of sediment loads show the greatest impacts, with potential reductions of up to 97.6 and 80%, respectively, from pre-dam conditions. In some development scenarios, the amount of water regulated and withheld by upstream infrastructure is of similar magnitude to existing fluxes involved in the episodic inundation of the floodplain during dry years and, thus, can also induce substantial changes in floodplain seasonal dynamics of average-to-dry years in some areas of the Mompós Depression.

Keywords: Cumulative impacts on freshwater systems, River fragmentation, Migratory fish, Floodplains dynamics, Sediment entrapment

1 Introduction

Hydropower is a fundamental component of many countries' energy supply due to comparative advantages such as long-term economic efficiency, flexibility to adapt to high-frequency demand fluctuations, and greater regulation of hydrologic variability for other water users. Recently, climate change considerations have reawakened interest in hydropower development for its potential contributions to low-carbon economies and reduced dependencies on fossil fuels.

Dam and reservoir construction and operations are one of the main drivers of global change in freshwater systems (Dynesius and Nilsson, 1994; Grill et al., 2015; Zarfl et al., 2014). There are numerous examples worldwide of how changes in flow, sediment, and temperature regimes; loss of river connectivity; and other impacts associated with reservoirs and dams cumulatively affect physical and ecological processes that determine the integrity of major river systems, and in particular, of riverine lowland floodplains and wetlands (Arias et al., 2014; Dang et al., 2016; Grill et al., 2015; Opperman et al., 2010; Tockner and Stanford, 2002).

Riverine floodplains and wetlands are ecosystems of high biodiversity and productivity (Tockner & Stanford, 2002), providing numerous benefits, including stable water supplies, support for fisheries, flood risk mitigation, carbon regulation, and improved water quality (Zedler and Kercher, 2005). Floodplain systems—despite their comparatively small spatial footprint—generally exceed the productivity of purely terrestrial or purely aquatic ecosystems (Bayley, 1995; Tockner and Stanford, 2002). Due to their central role in processes operating at the basin scale, and to the economic value of the numerous services they provide, hydrologically and ecologically functional riverine floodplains should be considered in sustainable water management infrastructure development. Such considerations should go beyond project-scale environmental impact assessments to consider the cumulative effect of all interventions located upstream (Dang et al., 2016; Fitzhugh and Vogel, 2011; Yang and Lu, 2014).

Basin-scale analysis aims to explicitly take into account the benefits of water management infrastructure along with potential repercussions to long-range processes and services that freshwater systems naturally provide; such analysis is especially relevant because the hierarchical and nested character of river networks and their associated ecosystems lead to non-linearity of impacts (Fullerton et al., 2010; Grill et al., 2015). For example, habitat fragmentation is highly dependent on the geographic configuration of artificial barriers (Fausch et al., 2002); unique disturbances at specific locations can have system-wide impact, and multiple dams, while individually disconnecting relatively small parts of the river network, can together disconnect large portions of non-substitutable habitat, constraining key ecological or physical processes, like fish migration from floodplains to upstream spawning habitats, or sediment and nutrient transport (López-Casas et al., 2016; Yang and Lu, 2014).

Floodplains and associated wetlands rely on longitudinal, lateral, and vertical connectivity which all affect the extent, depth, duration, and frequency of inundation. Cumulative flow alteration associated with upstream reservoir operation disrupts

these hydrologic processes, which, in turn, affect multiple physical and ecosystem characteristics and processes, like floodplain topography; deposition of nutrients and organic matter in the floodplain; recharge of the water table; recruitment, dispersion, and colonization of plants; triggers for fish migration; and access to soil moisture, among many others (Arias et al., 2014; Poff and Zimmerman, 2010).

Like habitat fragmentation, changes in the magnitude, frequency, duration, and timing of river flows also exhibit non-linear cumulative behavior (Dang et al., 2016; Poff et al., 1997; Richter et al., 1998). While the artificial regulation effect of individual dams on hydrologic alteration depends both on reservoir storage capacity in comparison to the natural river discharge and on the operational rules (Williams and Wolman, 1984), at the basin level, dam placement determines both the spatial extent and the degree of alteration; certain relative dam locations can enable (or preclude) attenuation of streamflow from tributary rivers, and multiple dams located in the same river branch or sub-basin can amplify the artificial regulation—resulting in hydrologic alteration greater than the sum of the individual effects of single reservoirs—propagating impacts hundreds or thousands of kilometers downstream (Angarita et al., 2013; Fitzhugh and Vogel, 2011; Piman et al., 2016; Richter et al., 1998).

The decrease in sediment loading due to reservoir trapping is another important driver of change in freshwater systems (Vörösmarty et al., 2003). Deficits in sediment loads are responsible for a number of impacts, like erosion and subsidence of river deltas (Syvitski et al., 2009), progressive incision or incremental changes in channel sinuosity and bank erosion (Grant et al., 2003), and transformation of wetlands and floodplains into permanent water bodies; and indirectly, as consequences of these impacts, de-stabilization of infrastructure like bridges, bank protections, levees, etc.

Medium and large hydropower plants in the Magdalena River basin (MRB) with a total capacity of 6.89 GW currently supply 49% of the electricity consumption in Colombia. Faced with growing demand—by 2050, electricity use in Colombia is expected to increase by between 105% and 147% with respect to 2010 (UPME, 2015)—there is great interest in further developing the remaining MRB hydroelectric potential, estimated at ~35 GW (Departamento Nacional de Planeación, 1979). Due to its proximity to existing transmission infrastructure and to urban areas that represent 75% of the energy demand of the country, the Magdalena River and its tributaries make an attractive target for further hydropower expansion. Recently, basin-level impacts of MRB hydropower have been discussed in terms of a) cumulative hydrologic alteration (Angarita et al., 2013); b) loss of longitudinal connectivity (Opperman et al., 2015); c) contribution to changes in fish productivity, extinction risk, species distribution, community composition, and extent of spawning habitat (Carvajal-Quintero et al., 2017; Jiménez-Segura et al., 2014; Pareja-Carmona and Ospina-Pabón, 2014); and d) reproductive biology of fish of economic importance (López-Casas et al., 2014, 2016; Villa-Navarro et al., 2014).

However, none of the above-mentioned studies included an integrated basin-level analysis of cumulative impacts on lowland riverine floodplains in the MRB. In this paper, we present an assessment of the current and potential basin-scale impacts of hydropower expansion on these floodplains—the Mompós Depression wetlands. We propose an integrated framework that takes into consideration basin-level and local factors to assess system alteration. From a basin-level perspective, we first developed an integrated analysis of three main factors associated with cumulative impacts of hydropower infrastructure:

flow regime alteration, sediment trapping, and connectivity losses with upper tributaries, with an emphasis on migratory fish species. Second, to estimate long-range hydrologic dynamics of floodplains, we developed an enhancement of the Water Evaluation and Planning system, or WEAP (SEI, 1992-2017), capable of reproducing floodplain fluxes and storage, to resolve the Mompós Depression floodplains' water balance at a medium scale (~1000 to 10 000 km^2) and evaluate its relationship to upstream and local water management.

2 System description

The Magdalena River is located in the Northern Andes Mountains and drains a biodiverse mosaic of ecosystems along its journey northward to the Caribbean Sea. The basin covers nearly one quarter of Colombia's national territory, providing sustenance, and acting as an economic and cultural life-force, especially for the more than 35 million Colombians—70% of the country's population—who live within its bounds (Figure 1).

With a length of 1540 km, the main stem of the Magdalena is the principal riverine trade artery of the country and the main connection to the Atlantic Ocean (ARCADIS Nederland BV and JESYCA S.A.S., 2015). Following the Strahler system of stream order classification (Strahler, 1957) the MRB network ranges from small mountain tributaries (order 1), to the Magdalena at its mouth in the Caribbean Sea (order 8). The total network comprises a total length of approximately 101 109 km of which 11 997 are medium to large rivers (Strahler order ≥4). Average flows range from 46 ± 30 m^3/s (order 4 rivers) to 7359 ± 203 m^3/s (order 8).

The Magdalena River flows between the Eastern and Central Cordillera of the Northern Andes. Tanner (1974) argued that the Magdalena River valley is an "incomplete flood plain", a term he defined in a submission by the same name. Floodplain incompleteness, according to Tanner, can result either from rapid changes in sea level or from continued tectonic deformation, the latter being a likely explanation in this intermontane basin within the active Andes orogenous zone. Incomplete floodplains are characterized by lakes, marshes, wetlands, and swamps—depressions inundated by a high water table—and lack signs of prior meandering or channel migration. Near the town of El Banco (23.5 masl), situated just upstream of what is considered the lower Magdalena, the Magdalena River is joined by the Cesar River. Downstream of El Banco, it splits into numerous channels, and is joined by two more tributaries: the Cauca and the smaller San Jorge (Figure 1). The tectonically active foreland basin of the lower Magdalena "consists of vertically accreting, levee-confined channels and adjacent extensive [Mompós] wetlands, which are interpreted as an anastomosing river sedimentary system" (Smith, 1986, p. 177). A notable feature of this basin is extensive and water-logged negative-relief elements (Lewin and Ashworth, 2014). The wetlands, dissected by numerous tie-channels, together with the permanent and temporary lentic waterbodies called "ciénegas" encompass approximately 3400 km^2, comprising one of the largest wetland systems in South America. About 200 km from the Caribbean Sea, downstream of the city of Mangangué (10 masl), the numerous braids of the Magdalena converge and meander as a single channel until the Magdalena splits again at Calamar, with part of the flow diverted westward to Cartagena through an altered channel system that serves as a navigation canal and part flowing into a 100-km long delta, while the main river continues to its mouth in Barranquilla.

The Magdalena is among the rivers with the highest sediment yields in South America: 560 t/km²/year—a rate approximately three times that in the Amazon, La Plata, and Orinoco rivers (Restrepo, Kjerfve, Hermelin, & Restrepo, 2006). The most recent estimate of annual sediment flux (suspended sediments) of the Magdalena is 142.6×10^9 kg yr^{-1} (Restrepo, Ortíz, Otero, & Ospino, 2015). High rates of sediment transport have shaped the basin-scale morphologic and hydrologic dynamics that determine the complex storage and exchange patterns of water in the river and adjacent plains (Posada G. and Rhenals, 2006).

The discharge pattern of the Magdalena to the Mompós Depression is largely determined by the Inter Tropical Convergence Zone, which annually oscillates from the equator to the northern Andes and back, resulting in two rainy seasons: April-May and September-November (Poveda et al., 2011). This weather pattern typically results in predictable bimodal discharge peaks in April-May and October-November (Poveda et al., 2001; Smith, 1986). The roles of topography, soil-atmosphere interactions, the Atlantic Ocean, and the Amazon also influence temporal and spatial rainfall patterns, resulting in the bimodal character not being equally strong across the basin (Poveda et al., 2011). The lower basin near the Caribbean coast—including the Mompós Depression—is often suggested to be unimodal in character, and the southeastern portion of the basin (approximately below 2°N) is characterized by a distinct unimodal pattern, with a June-to-August wet season (IDEAM, 2014).

During intense El Niño-Southern Oscillation (ENSO) events, the ITCZ can extend anomalously far south bringing drought conditions in the MRB. In contrast, during La Niña events the MRB experiences heavier than normal rains and colder conditions that often extend—sometimes even bridging ITCZ events, leading to rainy periods that can last a year or longer (Poveda et al., 2001; Poveda and Mesa, 1997). The strong relation between anomalously high or low stream flow conditions at four stations in the MRB and the Oceanic Niño Index, a measure of ENSO, is illustrated in Figure 2. Observed climate variability in the MRB also exhibits oscillations at decadal or interdecadal timescales, represented by multiple macroclimatic oscillations including Pacific Decadal Oscillation and Atlantic Multidecadal Oscillation (IDEAM, 2014).

The hydrologic variation of the lower Magdalena River and its resulting hydroperiod in the Mompós wetland system are crucial to the system's high ecological complexity and species diversity. The wetland ecosystems depend on seasonal inundation and the nutrients and sediment delivered by floodwaters. The system contains more than 226 native fish species with 129 (57%) endemic (Maldonado-Ocampo et al., 2008), and at least 16 that undertake reproductive migration from the low floodplain to the foothills of the Andes (López-Casas et al., 2016). This richness and high species endemism, in addition to the proximity to main human settlements, has made the river the country's main and most productive fishery, one based on at least 40 species (FAO, 2015). Fish are the main source of dietary protein for many MRB communities (Galvis and Mojica, 2007; Lasso et al., 2011). Additionally, the wetlands and lagoons of the lower Magdalena are critical stopovers for migrating and wintering birds along the Pacific Americas Flyway, where episodic inundation is critical to fish and bird reproduction, while low-flow conditions are important for reptile reproduction, propagation of riparian flora, and nutrient and organic matter storage (Jaramillo et al., 2015).

3 Data and methods

3.1 Basin-level considerations

3.1.1 Defining dam sets for current and potential development

This study focused on existing and proposed medium and large hydropower projects, including reservoirs and run-of-river plants. Such projects can reduce river network connectivity or produce downstream alterations. Currently the MRB upstream of the Mompós Depression provides 70% of Colombia's hydropower, equivalent to 49% of the country's electricity supply (XM, 2014). Ninety-five percent of the capacity is distributed over 35 plants (32 in operation and three expected to be completed in 2018), with an aggregate installed capacity of 6.89 GW (and expected expansion to 9.35 GW in 2018) and 17.2 billion m^3 of storage (equivalent to 8.4% of the basin's average annual runoff). The remaining 5% corresponds to small hydro plants (< 20 MW).

In Colombia there is no centralized or coordinated planning for hydropower site identification; expansion occurs on an individual project basis in response to rolling auctions issued by the government based on 5- to 15-year projected needs of additional generation capacity (Cramton and Stoft, 2007; UPME, 2012).

To account for this uncertainty, our analysis first identified and compared a set of 1000 possible future scenarios—starting from a baseline condition that includes existing and under-construction dams—using a catalog of 97 potential project sites identified in Colombia's 1979 hydropower inventory (Departamento Nacional de Planeación, 1979) (Table 1), considered to be reliable by government and developers (See locations in Figure 1). We evaluated each scenario with respect to cumulative basin-level impacts of a) loss of river network longitudinal connectivity between wetlands and upstream tributaries, b) boundary conditions of flow regime alteration, and c) loss of sediment input due to reservoir entrapment. A second set of scenarios was then generated by applying restrictions. Based on results from the first 1000 scenarios (grey dots in Figure 8), we created four additional sets of 100 scenarios each. Each set is a randomly sampled subset of projects (colored dots in Figure 8) that avoid one or more criteria—projects located on Mompós Depression tributaries (order 4+) not yet affected by artificial barriers, mainstem projects upstream of existing projects, projects that would inundate areas with > 300 inhabitants, and projects that would inundate productive lands > 300 hectares. In the context of Colombia's regulatory framework for energy expansion, this second set of scenarios demonstrates some examples of the sensitivity of developable hydropower potential to basin-level policy for site identification guidelines

From the subset of scenarios that meet projected hydropower expansion by year 2050—an equivalent hydropower capacity of 15.25±0.5 GW, or +125% with respect to 2010 (UPME, 2015)— we selected five scenarios representative of the range of impacts and trade-offs in the basin on which to perform a more detailed analysis of the potential changes in streamflow regime and hydrologic dynamics of the Mompós Depression wetlands. This analysis consists of a 33-yr simulation of reservoir operations (using as reference the period 1981 to 2013). The simulation results allowed us to estimate the potential changes in streamflow regime and hydrologic dynamics of the Mompós Depression wetlands associated

3.1.2 Flow regime alteration

As part of this study, we developed a new indicator, named the *weighted degree of regulation (DOR_w)*, to perform a comparative analysis of potential cumulative impacts of the natural flow regime of multiple reservoirs at the level of an entire river basin. The indicator is based on the original DOR, applied in several regional and global assessments as a first-level approximation of flow alteration (Grill et al., 2015). DOR_w is defined as the relationship between the cumulative reservoir storage upstream and the total annual river flow in a river section, weighted by the percentage of upstream runoff effectively controlled by artificial storage, or:

$$DORw_r = \frac{Q_{cr} \cdot \Sigma_{upstream_r} V}{Q_r^2} \cdot 100\% \quad (1)$$

where Q_c is the upstream annual runoff affected by artificial storage, V the reservoir volume, and Q the total annual river runoff, with the r sub-index referring to specific reaches. Higher values indicate a greater potential alteration of the natural flow regime—particularly of seasonal patterns—due to operations effects of the reservoirs. In comparison with the previous *DOR* index, DOR_w provides a better estimate of the non-linear effects of attenuation of artificial regulation, by explicitly considering both the fraction of basin runoff not affected by reservoir operations and the distribution of artificial regulation across different rivers in comparison to regulation located in a single river. As DOR_w provides a basin-scale index of basin-level flow alteration it is thought to be particularly useful as a metric for basin-scale impacts on downstream wetland systems as found in the Mompós wetlands.

For the five selected scenarios of hydropower expansion thought to be representative of the potential range of alteration, we performed a 32-year simulation of the system to estimate boundary conditions (monthly streamflow) at the three main tributaries upstream of the Mompós Depression—the Magdalena, Cauca, and Nechí rivers—using Matlab's *ReservoirSimulator* model (Angarita et al., 2013; Ritter, 2016). This model performs a water balance of the inflows from tributary sub-basins of the reservoirs, coupled to a reservoir operations routine for hydropower production, along with other requirements such as water diversions and environmental flow obligations, when applicable (see SI-1).

For a given reservoir, the model takes into account physical and technical constraints, such as volume-elevation curve, tail-water elevation, operational levels (inactive, buffer, technical, and safety), turbine type, capacity, and efficiency. Physical characteristics for existing dams were obtained from project official documentation archives, and for projected dams from the 1979 inventory (Departamento Nacional de Planeación, 1979). MRB river topology, sub-basins, and volume-area-elevation curves were derived using the HydroSHEDS, dataset (Lehner et al., 2008; Lehner and Grill, 2013). Unimpaired flows for each sub-basin were lumped at dam sites based on observed runoff records from 1981 to 2013.

Water allocation for hydropower is based on basin-level target generation for a given time step. Target-generation for a multi-reservoir system is an extremely complex problem, subject to many interlinked factors operating at multiple time-scales, including water inflows, operational rules and technical constraints, firm energy obligations, fuel prices, and energy market competition (Cramton and Stoft, 2007; Ritter, 2016). In order to provide a plausible estimate of the monthly variability of generation targets of hydro-plants in the MRB, we evaluated the historical monthly average plant-factor (PF;

Figure 3)—the average percentage use of installed capacity—of existing medium and large hydro plants in the MRB from 2000 to 2015, based on market data (XM, 2014). Monthly average PFs for the MRB range from 41 to 85%; with most of the variation associated with hydro-climatic oscillations, like the 2008-2011 sequence of Niña-Niño-Niña events (Figure 2). On the other hand, intra-annual monthly variation of PF in non-extreme years shows relatively stable values within a year, with a variation of 10-16% from dry to wet months. This is consistent with the prominent role hydropower plays in Colombian energy supply and base-load generation; cumulative storage and water allocation is able to compensate—on a monthly basis—for seasonal hydrologic variability. Based on observed PFs, we developed the following regression model to estimate average monthly PFs for the full simulation period 1981-2013 (Adj R^2=0.62, Std. error=5.8%):

$$\mathrm{PF} = -0.031 \cdot \mathrm{ONI} + 1.205\times10^{-5} \cdot \mathrm{QL}_{\mathrm{Calamar}} + 0.233 \cdot \mathrm{Log}\left(\mathrm{MA}_6(\mathrm{QL}_{\mathrm{calamar}})\right) - 0.371 \quad (2)$$

where *ONI* is the Oceanic Niño Index, $QL_{Calamar}$ the monthly average streamflow at Calamar (station 2903702, shown in Figure 2), and MA_6 a moving average operator applied over a six-month period.

3.1.3 Sediment trapping

We estimated basin-level entrapment or S_e, defined as the percentage of total sediment throughput retained by upstream reservoirs, considering two main factors: individual reservoirs' retention efficiency, and the relative locations of multiple upstream reservoirs.

To estimate trapping efficiency for each reservoir, we used Dendy's formula (Dendy, 1974). Dendy's method is a revised Brune curve, which uses an empirical expression to estimate the long-term average reservoir sediment retention efficiency based on the ratio between capacity (*C*) and average annual inflow (*I*). A higher ratio indicates higher sediment retention efficiency, *TE*, as described by the following equation:

$$TE = 100 * \left(0.97^{0.19^{Log\left(\frac{C}{I}\right)}}\right) \quad (3)$$

Similar to the case of flow regime alteration, relative locations of reservoirs play an important role in sediment entrapment because upstream reservoirs can significantly reduce sediment input to downstream reservoirs, and sediment yields vary across the basin (See Restrepo et al., 2006, for a detailed analysis of the MRB). To consider the effects of relative dam locations and of sediment yield heterogeneity, we developed a routing model for reach-level sediment balance, as described by the following recursive equation:

$$SST_r = \left(\sum_{u \in \boldsymbol{Inflow_r}} SST_u + E_r * A_r\right) * (1 - TE) \quad (4)$$

where SST_r is the sediment load downstream of reach *r*, $Inflow_r$ the set of river reaches directly upstream of reach *r*, A_r the drainage area, and E_r the contribution of sediments generated by laminar erosion and storage on the slopes, based on the Revised Universal Soil Loss Equation (RUSLE) methodology:

$$E_r = R \cdot K \cdot L_s \cdot C \cdot P \quad (5)$$

where *E* is the laminar erosion [ton/m^2/year], *R* rain erosivity [MJ mm/m^2/h], *K* soil erodability [ton·h/MJ·mm], L_S topographic factor [dimensionless], *C* soil cover [dimensionless], and *P* management practices [dimensionless]. Values for

each of the corresponding variables were adopted from Jimenez (2016) for the MRB. Our simplified approach focuses on the primary inputs and outputs in a section of a stream according to Wilkinson et al. (2009), where the primary production process corresponds to the contribution of slope and channel erosion in the upper parts of the basin (Strahler order 1). Our main purpose was to provide a basis for comparative analyses of sediment retention in the tributary rivers of the Mompós Depression for the different hydropower expansion scenarios; therefore, we do not provide a comprehensive description of the other components of the channel sediment balance, such as sediment production by lateral migration of the channel, or bank overflow events and sediment deposition.

3.2 Floodplains hydrologic dynamics

We developed a conceptual hydrological model with a surface storage component that includes episodic interactions between river and wetland systems as an enhancement to the WEAP platform's existing Soil Moisture Model (SMM) (Yates et al., 2005b). The model dynamically simulates evapotranspiration, surface runoff, sub-surface runoff or interflow, and deep percolation at the sub-basin level, as well as bi-directional water transfer between river and wetland systems. The water balance is defined using a semi-distributed approach that reflects the topological relationships between basin areas or catchments, stream networks, and wetlands. The model allows for the evaluation of hydrologic dynamics associated with several factors, including alteration in the upstream flow regime, climate variability and change, and impacts of local and upstream water resource management practices, such as flood control structures and changes in connectivity between river and wetland systems.

WEAP SMM enhancements included two main modifications: the inclusion of surface storage for water balance representation at the catchment level; and the topological representation of interactions between surface storage, sub-surface storage, and the river network. WEAP's original SMM represents the water mass balance through two soil layers—the root zone and the deep zone—in lumped portions of the watershed called catchment objects, each divided into *N* fractional areas *j* representing different land cover types, with a water balance computed for each fractional area. The model "uses empirical functions that describe evapotranspiration, surface runoff, sub-surface runoff or interflow, and deep percolation" (Yates et al., 2005a, p.491). The modified version introduces a third storage volume (or "bucket"), corresponding to a fractional area of the catchment that accounts for surface storage. The water balance in the third bucket is determined by a) bidirectional exchanges of water (flood and return flow) with one or more sections of river and b) local inputs-outputs such as precipitation, evaporation, or percolation (Figure 4).

Water balance in the soil root zone and soil deep zone are calculated, respectively, by land cover type:

$$Sw_j \frac{dz_{1,j}}{dt} = P + Ir - PET * k_{c,j}(t)\left(\frac{5z_{1,j} - 2z_{1,j}^2}{3}\right) - (P_e + I_r)z_{1,j}^{RRF_j} - \left(1 - f_j\right)k_s z_{1,j}^2 \quad (6)$$

$$Dw_j \frac{dz_{2,j}}{dt} = \left(1 - f_j\right)k_s z_{1,j}^2 - k_d z_{2,j}^2 \quad (7)$$

The total runoff (*Ro*) [volume] and baseflow (*Bf*) [volume] of a given catchment is then calculated as the sum of the contributions of the land cover types:

$$Ro(t) = \sum_{j=1}^{N} A_j \left[(P + Ir) z_{1,j}^{RRF_j} + f_j \, k_s \, z_{1,j}^2 \right] \quad (8)$$

$$Bf(t) = \sum_{j=1}^{N} A_j \left[k_d \, z_{2,j}^2 \right] \quad (9)$$

where

Sw_j soil root zone water storage capacity (length),

Dw_j deep zone water storage capacity (length),

z_1 water stored in the root zone, relative to its total storage capacity (%),

z_2 water stored in the deep zone, relative to its total storage capacity (%),

P precipitation and snowmelt in the catchment (length),

Ir irrigation (length),

PET Penman-Monteith reference crop potential evapotranspiration (length time^{-1}),

$k_{c,j}$ crop coefficient (dimensionless),

f_j flow direction (dimensionless),

k_s conductivity of the root zone (length time^{-1}),

k_d conductivity of the deep zone (length time^{-1}),

RRF_j runoff resistance factor (dimensionless), and

A_j area of land cover type j

Likewise, the mass balance at the floodplain and the connected river reaches (V_{river}), is represented by:

$$\frac{dV_{3,j}}{dt} = Q_l - R_l - A_3 * \left[P_e * z_{1,j}^{RRF_j} - PET(t)(1 - k_{c,j}) \left(\frac{5z_{1,j} - 2z_{1,j}^2}{3} \right) \right] \quad (10)$$

$$\frac{dV_{river_i}}{dt} = Q_h - Q_l - Ir + R_l + Ro + Bf \quad (11)$$

where

$V_{3,j}$ storage volume in the floodplain (volume),

$V_{river,i}$ water stored in the connected river reach (volume),

A_3 extent (area) of flooded area, given the volume of floodwater in catchment,

Q_h river reach input streamflow,

Q_l lateral flow between river and floodplain (volume time^{-1}), defined as percentage T_f of the river reach streamflow, above a certain flow threshold:

$$Q_l = \begin{cases} T_f \cdot (Q_h - Q_{threshold}), \; if \; Q_h > Q_{threshold} \\ 0, \; if \; Q_h < Q_{threshold} \end{cases} \quad (12)$$

and R_l return flow from floodplain to river reach (volume time^{-1}), defined as the percentage T_r of water above a floodplain storage threshold, that flows out of the floodplain in one time step:

$$R_l = \begin{cases} T_r \cdot (V_3 - V_{3,threshold}), if \; Q_h < Q_{threshold} \\ 0, if \; Q_h < Q_{threshold} \end{cases} \quad (13)$$

While there is a wide range of modeling approaches to study floodplain systems dynamics, including MIKE21 (DHI, 2016), ANUGA HMP (Roberts, 2006-2017), and HEC-RAS (USACE and RMA, 2016), conceptual approaches have several advantages, as previously discussed by Dutta et al. (2013). Our lumped-topological model has fewer information requirements and a much shorter execution time than a hydrodynamic model. Therefore, the approach is suitable for the simulation of long periods of time, and for comparative analysis of multiple scenarios for planning and management. Also, this type of model allows for long-term evaluation of floodplain dynamics and broader potential management implications.

The WEAP enhancements were developed for the Mompós Depression and adjacent lowland basin, with a total area of 32 198 km², or 11.8% of the total area of the entire MRB. The area receives flows from the Magdalena, Cauca, San Jorge, and Cesar rivers (Figure 1 and 5). Catchments were determined by selecting basin-scale natural "breaks" in river system topology to allow the identification of basins, inter basins, and internal basins based on the Pfaffstetter hierarchical basin coding approach (Verdin and Verdin, 1999), implemented in the recently released HydroBASINS product (Lehner and Grill, 2013). Comparison of the hydrographic units with the basin morphogenic classification (IDEAM, 2010), revealed a strong coincidence between these units. This is consistent with morphogenic classification being conditioned by factors such as geologic structure, bioclimatic conditions, topography, and slope. Land cover classification is based on seven differentiated categories in terms of their physiognomy: Forests, Shrubs, Grasslands, Agricultural Zones, Water bodies, Hydrophytes and Others, which were derived from Colombia's ecosystem map (IDEAM et al., 2007).

3.2.1 Topological representation of the floodplains system

Using WEAP's semi-distributed modeling approach, Equations 6 to 11 can be set independently for multiple river reach and floodplain connections, allowing for the representation of complex topological relationships between catchments, river reaches, and floodplains (Figure 5). For example, a floodplain fed by the overflow from multiple river reaches, and the distribution to multiple reaches of the floodplain's return flow can both be represented.

In practice, most of the model catchment sub-units are described only by Equations 6 and 7, representing areas of the basin not subject to flooding. For the subset of catchments that represent floodplains (as shown in Figure 5), the model is set up to include Equations 10 and 11. To reduce the number of model calibration parameters, topological connections between the river and floodplains were pre-identified using multiple sources of contextual information. In the case of the Mompós Depression, clues for permanent and episodic connectivity were derived from a review of remote sensing data (Landsat 5, 7, and 8) over time and of topological data derived from a high-resolution DEM recently developed by Colombia's [Climate] Adaptation Fund in the area between the Cauca and San Jorge rivers, as documented by Sanchez-Lozano et al. (2015).

3.2.2 Model calibration, validation, and uncertainty estimation

The WEAP model was calibrated (1981-1998) and validated (1999-2013) for monthly streamflow at 13 discharge gauges and for water level at four stations with long-term records in the Mompós Depression (Figure 1). Historical monthly precipitation, temperature, discharge data (m^3s^{-1}), and water levels (m) were obtained from Colombia's National

Meteorology, Hydrology, and Environmental Studies Institute (IDEAM). The longest available records date back to 1940 for station QL (2903702, Calamar), located at the outlet of the Mompós Depression (Figure 1). Other stations provide relatively high serial-complete streamflow records starting in 1972.

We adopted Nash Sutcliffe Efficiency (NSE) and Relative Bias (P-BIAS) for streamflow data, and R^2 between wetland water levels and storage as orthogonal performance metrics; in the case of wetlands, a correlation between water levels and storage was adopted due to a lack of topo-bathymetrical data, which prevented the conversion of the model state variable (storage volume) to effective water levels in wetland units. Despite this limitation, the R^2 metric reflects the model's ability to capture the dynamic character of water levels in wetland areas.

In both cases, acceptance ranges were chosen based on Moriasi et al. (2007). Model parameters (54 in total) were then calibrated using a three-stage random hypercube sampling. The first stage was derived from 10 000 simulations and the subsequent two were derived from 1000 simulations each. Sets of model parameters above acceptance criteria ranges of the 30-simultaneous metrics (13 NSE, 13 P-BIAS, and 4 R^2) were used to assess model uncertainty by analyzing the range of predicted average and maximum floodplain storage.

3.2.3 Hydrologic alteration of floodplains

One of the most widely accepted methodologies to assess the impact of changes of flow regime on aquatic ecology is the concept of Indicators of Hydrologic Alteration (IHA), as proposed by Richter et al. (1996). IHA is a set of 32 statistics related to magnitude, timing, duration, frequency, and rate of change, which allows a detailed comparative analysis of diverse flow components. Many of the statistics are inter-correlated, rendering part of this vast amount of information redundant for high level assessments (Gao et al., 2009; Vogel et al., 2007). In order to simplify IHA, Gao et al. (2009) demonstrated that "Ecodeficits" and "Ecosurpluses" (EDS), defined as relative changes of flow duration curves can provide a comprehensive simplified representation of hydrologic alteration impacts, as compared with the use of the more complex IHA approach.

In this study we employed seasonal EDS to assess the impact of variations in the hydrologic regime of wetlands storage. We divided the year into four seasons: *Subienda* (Dec–Feb), *Bajanza I* (Mar-May), *Mitaca* (Jun-Ago), and *Bajanza II* (Sep-Nov); these periods were selected based on their biologic and hydrologic relevance in the basin, in particular to fish migration, as in Jiménez-Segura et al. (2014). We differentiated ranges of duration corresponding to storage magnitude for: extreme high (months with *percentage of time exceeded <10%: Max* to *P10*), seasonal (*P10* to *P75*), low (*P75* to *P90*), and extreme low flows (*P90* to *Min*), also relevant to diverse ecological processes (DePhilip and Moberg, 2013).

3.2.4 Habitat fragmentation in the upstream tributaries

We estimated fluvial length loss over the gradient 0 to 3000 masl, with a focus on reaches used by species of migratory fish present in the Mompós Wetlands. Loss of river length is a proxy for fractionation of populations and communities, and for

reduction or isolation of available habitat necessary for the different life stages of species and/or groups with specific distribution ranges (Carvajal-Quintero et al., 2017; Fullerton et al., 2010).

We used biological data derived from Species Distribution Models (SDMs) fitted with MaxEnt v3.3.4 for 13 of the 16 species in the MRB known to migrate upstream from the floodplains: *Brycon henni, Brycon moorei, Curimata mivartii, Cyphocharax magdalenae, Leporinus muyscorum, Pimelodus blochii, Pimelodus grosskopfii, Plagioscion magdalenae, Prochilodus magdalenae, Pseudoplatystoma magdaleniatum, Saccodon dariensis, Salminus affinis,* and *Sorubim cuspicaudus*. Fish records consist of information available in principal ichthyological collections and surveys of migratory fish since 1940, which provide information on the historical distribution of fish in the MRB prior to hydroelectric development. A total of 31 environmental variables describing climate, soil, and geomorphology were considered. Principal Component Analysis (PCA) between those variables were used in SDMs to avoid multicollinearity. An "All Target Group" approach was used in SDMs to reduce error associated with sampling bias (Phillips et al., 2009). To evaluate model performance, we used the mean value of the area under the curve from the receptor of operator characteristic resulting from ten random cross-validation sets (70% of data for calibration and 30% for testing). The threshold that maximized the sum of specificity and sensitivity resulted from cross-validation and was used to obtain fish distributions in presence-absence format (Liu et al., 2013).

To perform connectivity analysis using the topological river network, we assigned SDMs as an attribute (presence-absence) to each river reach; as a result, a total of 11 434 km of medium and large rivers (Strahler order 4 or higher) were found to be historically associated with one or more migratory species. Migratory fish habitats are predominantly located below 1000 masl (9371 km; 85.1% of the total river network). To account for the different elevation ranges associated with different life stages of migratory fish —*Pseudoplatystoma magdaleniatum* and *Sorubim cuspicaudus* do not exceed 500 m; *Pimelodus grosskopfii* can reach 900 m; *Prochilodus magdalenae, Salminus affinis,* and *Brycon moorei* are reported to perform reproductive migrations up to elevations of 1500 m; and *Brycon henni* can reach 2000 m (Jiménez-Segura et al., 2014)—we evaluated the total loss of connectivity in three elevation ranges: 0 to 400 masl (juvenile fish growth), and 400 to 1000, and 1000 to 1500 masl (migration and spawning).

4 Results

4.1 Upstream impacts

4.1.1 Baseline conditions

The baseline length of the river network associated with migratory fish (Strahler order ≥4) and connected to the floodplains is 6789 km in the elevation range of 0 to 400 masl, 1104 km between 400 to 1000, and 123 km between 1000 and 1500 masl. Compared to a total pre-dam length of 11 434 km (6963, 2402 and 941 km, respectively, in the specified elevation ranges), this represents a loss of 28.8% of connected river length, with the greatest connectivity loss at high elevations: Only 2.5% of

the total river length is affected by fragmentation at 0 to 400 masl, while between 400 and 1000 masl the figure is 54.0%, and between 1000 and 1500 masl, 86.9% (Figure 6). Figure 6 illustrates the distinct differences in topographic profiles of the mainstem and its tributaries, and could be used to identify potential natural breaks in connectivity and local hotspots for endemism due to steep variations in gradient. Altitudinal distribution of fish species and habitat loss with increasing elevation is shown in Figures 6d and 6e.

The baseline cumulative hydrologic alteration—expressed as DOR_w— is 3.2%; At Peñoncito station on the Magdalena River (2502733), La Coquera station on the Cauca (2624702), and La Esperanza station on the Nechí (2703701) shows relatively low levels at 5.2, 3.0, and 3.2%, respectively, but with high levels of controlled runoff: 48, 80, and 25%, respectively (Figure 7a). Current low levels of regulation are explained by the comparatively low storage capacity of existing reservoirs in comparison with basin flows. However, sediment loads are estimated to have been reduced due to reservoir trapping of 40.9, 61.3, and 39.9% at the three locations, respectively (Figure 7b).

4.1.2 Future scenarios

Figure 8 presents the expected cumulative impacts of 1400 generated future scenarios (1000 randomly generated, and 400 following 4 sets of potential basin-level restrictions), highlighting those in the range of projected expansion by 2050 (15 250±500MW). Scenarios show wide ranges of increased impacts due to non-linearity. Regarding river fragmentation (Figure 8a), 6763 to 4391 km of connected river length between 0 and 400 masl remain in the different scenarios (a loss of 2.9 to 36.9% from pre-dam conditions). The range of potential loss of connectivity in elevations between 400 and 1000 masl is particularly dramatic, with outcomes between 1104 and 68.5 km of remaining connected network, a 15-fold impact range. The worst-case scenario (equivalent to a loss of 97.1% with respect to pre-dam conditions) would eliminate virtually all connections between lowland floodplains and upstream spawning areas, while the best-case scenario has no additional impacts to baseline condition. Figures 8b and 8c present downstream impacts of hydrologic alteration and sediment trapping, respectively. The expected range of basin-level cumulative DOR_w is 4.1 to 18.1%, equivalent to 1.3 to 5.7 times baseline condition. Ranges of DOR_w additional impacts also vary substantially between the Magdalena and the Cauca, being much higher in the latter. While this is mostly a result of the relative size of Magdalena in terms of flow (the Magdalena is approximately twice the size), it is worth to note that most of the largest reservoirs projected in the basin are located in the Cauca River, characterized by a much narrower and steeper river valley. Cumulative sediment trapping lies in the range of 41.0 to 68.9%, representing an additional change of between 1.1 and 29% over the baseline (39.9%).

Figure 8, also allows comparison of the range of basin-level impacts resulting from scenarios derived from the proposed sampling strategies. In this case, we did not attempt to explore comprehensively how different criteria can enable better outcomes. Rather, we illustrated how a potential application of a bottom-up approach of providing key information to decision makers in the basin could enable local and individual decisions (i.e. site selection, project size, etc) that "scale-up" to better basin-level outcomes. As shown, in some cases simple restrictions result in expansion pathways consistently better

in most of the analyzed impact and benefits metrics. Conversely, this type of analysis can illustrate that certain guidelines—while they may help avoid local impacts—are not sufficient to avoid basin-level impacts

There is a wide range of expected impact associated with scenarios of comparable hydropower capacity (Figure 9). Some trade-offs in the set can be clearly identified, such as regulation between the Cauca and Magdalena (we did not attempt to establish the pareto-optimal set, since the purpose of our study was not to perform an optimization). Through our analysis we found no statistically significant correlation between DOR_w and connectivity or between DOR_w and sediment trapping. This finding indicates the complementarity of the proposed metrics. In contrast, we found a high inverse correlation (R^2>0.84) between migratory connectivity and sediment trapping, indicating that future work could use sediment trapping as a proxy for connectivity loss, or vice versa. However, this relationship may be unique to the Magdalena system as some of the basin's migratory fish tend to migrate in tributaries that contribute significant sediment loads. It is worth noting that in all the scenarios considered additional regulation in the Cauca has little to no additional effect on sediment transport reduction; this is due to the high sediment trapping of the baseline condition, and specifically due to the high sediment retention efficiency of Projects 2 and 21. As a result, those projects will be subject to high sediment input that will affect their longevity.

The five selected scenarios (highlighted in Figure 9 and summarized in Table 2) are representative of the wide range of potential boundary conditions of the Mompós Depression: A and B are equivalent in terms of low sediment trapping and fragmentation of spawning habitats, but with contrasting geographical distribution of DOR_w. Scenario A adds artificial regulation in the Magdalena sub-basin, B to the Cauca sub-basin. C and E correspond to "mediocre" cases, while D was in the group of worst-case scenarios in terms of impact on artificial regulation, sediment load loss, and upstream connectivity. It should be noted that all five scenarios are plausible under Colombia's current regulatory framework.

Simulated average streamflow of the baseline and selected scenarios across stations 2502733 (Magdalena), 2624702 (Cauca), and 2703701 (Nechí) shows the two annual storage-release cycles (Storage: Mar-May and Sep-Nov, and Release: Dec-Feb and Jun-Aug), with consequent cumulative attenuation of the seasonal streamflow signal and the overall regulation effect of dry, average, and wet years (Figure 10). DOR_w levels as low as 10 to 15% (corresponding to scenarios A and C for the Magdalena and C for the Cauca), effectively reduce the amplitude of seasonal oscillations, especially in years with extreme dry macroclimatic conditions like 1992 and 1998 Niño events. Scenarios with higher DOR_w (>23%) (D for the Magdalena and Cauca, and B for the Cauca), can eliminate the seasonal signal altogether in average to dry years. None of the evaluated artificial regulation scenarios affects seasonal patterns or magnitudes during wet or extremely wet periods.

It must be noted that flow alteration impacts are highly influenced by operational rules, and even reservoir configurations with a high DOR_w can be operated to mimic the natural flow regime. While this study did not explore in detail the implications of alternative operational rules (our analysis only attempted to reproduce historical seasonal generation targets for the basin), the multiple simulations performed are representative of a wide range of DOR_w (from 3 to 29%) and can serve as a reasonable approximation of the envelope of expected operational behavior of multiple reservoirs with similar build-out storage capacities.

4.2 Floodplains analysis

4.2.1 WEAP model implementation

Figure 11 summarizes the model calibration and validation metrics for the sub-set of randomly generated model parameters (15 out of 12 000, 0.12%) with highest performance, above or closest to the acceptance ranges (NSE>0.65 and P-Bias<10%) —or "good-fit" model set. As shown, performance is consistent across the 13 streamflow gauges and calibration and validation periods, with the exception of streamflow gauges 2502749 and 2502757 (calibration). However, at the same locations, performance increases during the validation period (1999-2013), which may indicate errors in the observed record at those sites during the period 1981-1998. On the other hand, sharp performance decreases in gauges 2502720 and 2502764 are due to the Cauca levee breach that occurred during a 2010-2011 La Niña event.

Model sensitivity analysis of average and maximum volume storage in the main floodplain sub-units, shows results vary in the range of ±25% of the mean value of the set estimate in most of the sub-units, with the exception of C24 (Ciénaga de Ayapel), where observed variation of estimates was up to ±35% of the mean value of the subset of "good-fit" models.

Model limitations

The model developed runs on a monthly time step and represents large units. As a result, we were unable to evaluate high-frequency floodplain dynamics such as backwater effects on tributaries, and rates of increase in the depth and extent of flows. On the other hand, the extent of the flooded area was not directly reproduced by the model.

4.2.2 Hydrologic alteration of floodplain dynamics

Lastly, the new model allowed us to evaluate the potential changes in wetland hydrological dynamics for each of the considered configurations of hydropower in the MRB. Figure 12 shows the simulated changes for the baseline condition and for all hydropower expansion configurations aiming for hydropower production (A to E), and alternative operation schemes aiming to reduce peak flows during extreme high events (B' and D').

Results show a heterogeneous response of the different floodplain units to upstream hydrologic alterations; units with the highest sensitivity to increased DOR_w alteration are the Zapatosa, Rosario, Brazo de Loba, and Brazo Mompós, all of which are directly influenced by the Magdalena River. The Bajo San Jorge unit, which is influenced by the San Jorge, Cauca, and Magdalena, showed a comparatively lower sensitivity to upstream hydrologic alteration. The Ayapel and San Marcos units showed the lowest sensitivity to upstream alteration, consistent with the fact that the connection between the Cauca River and Ayapel and San Marcos floodplains became limited in the 1970s by the construction of a lateral levee west of the Cauca River (*Dique Marginal del Cauca*); currently those wetlands units are only influenced by the San Jorge River. Episodic levee failures, like the ones observed during the La Niña event of 2010-2011, have reestablished connection between the Cauca River and the San Marcos and Ayapel systems; however, such events during extreme wet periods are not affected by dam operations, as shown in the previous section.

Low and extremely low storage events showed the highest impacts from increased regulation of upstream tributaries. Under the baseline condition and all expansion scenarios, extremely low storage events (*P90* to *min*) are expected to have much higher magnitude and be much less variable, especially in floodplains with a permanent connection between the river and wetlands systems, like the Zapatosa, Rosario, Brazo Mompós, and Bajo San Jorge. Alteration is higher during the first half of the year, which typically oscillates with higher amplitude between dry and wet periods. Scenarios with the highest cumulative DOR_w at station 2502733 on the Magdalena River (Scenario D), also induced significant changes in the magnitude of low storage events (*P75* to *P90*), modifying the amplitude of seasonal variation of floodplain and wetlands storage. Low and extremely low storage events support biodiversity by enabling several ecological processes such as reptile reproduction, propagation of riparian vegetation communities, and nutrient and organic matter storage. Low storage also keeps invasive and introduced species in check by eliminating those that are not adapted to variable conditions.

Seasonal storage events corresponding to ranges of duration between *P10* and *P75* were found to change in floodplain units characterized by long periods of disconnection between floodplain and river systems, such as the Brazo Loba unit; with a higher sensitivity to seasonal ecodeficits in the range of *P10* to *P75* during the second half of the year, reduced seasonal storage in this area could have severe impacts on local ecosystem functioning, as episodic yearly inundation is critical for water, nutrient, and sediment delivery to the floodplain system. Connectivity times and storage volume also determine habitat availability for migratory and resident fish.

In scenarios with the highest cumulative DOR_w at station 2502733 (D), floodplain units with permanent connections like the Zapatosa, Brazo Mompós, and Rosario, also experienced small changes in storage in the range of *P10* to *P75*, and a reduction of small seasonal flood events, potentially affecting the extent of wetlands oscillation. Seasonal oscillation also supports multiple ecosystem processes, including prevention of the invasion of riparian vegetation into the channel, and a general contribution to habitat heterogeneity.

Regarding extreme high storage events, development of hydropower dams has very low impact on high flows/flood magnitude, as extreme high flows continue to occur even under alternative operation rules focused on increased buffer capacities for regulating extreme wet events (represented by scenarios B' and D'). None of the proposed scenarios would substantially reduce the magnitudes or duration of extreme floods associated with periodic high flow events (occurring every 10 years or more), such as those that occurred around La Niña in 2010-2011. Operation regimes aimed at maximizing energy production (maintaining higher storage to increase working head) as well as those aimed at reducing the magnitude of peak flows (maintaining lower storage to increase buffer capacity to store peak flows) show little-to-no effect on the magnitude of extreme high events. This is consistent with the fact that even at the highest *DORw* levels (up to 39.1% in the Cauca, or 24.7% in the Magdalena), usable reservoir buffering capacity during extreme wet events can be surpassed in less than two months at peak flow volume, rendering reservoirs unable to substantially affect the magnitudes of extensive wet seasons—like those experienced during 2010 and 2011—and forcing operators to spill water for dam safety. Nevertheless, extreme flooding events deposit nutrients and organic matter in the floodplain, recharge the water table, and determine geomorphologic dynamics of the system. However, as discussed in Section 4.1.2, proposed scenarios can also reduce

sediment loads up to 69%. Through reduced sediment loads during peak flood events, wetlands and floodplains could experience reduced productivity and a progressive transformation into permanent water bodies.

5 Discussion

5.1 Contributions of this research

From a general perspective, we believe this research can contribute to the adoption of effective frameworks for strategic decision-making in the configuration of hydropower expansion. Our research shows that integrated and basin-level considerations focused on cumulative impacts on long-range, key environmental processes and components can be effectively adopted as criteria for the multiple stages of hydropower planning and development, from site selection to identification of long-term expansion potential.

In this specific case, we focused our attention on key attributes of ecologically functional floodplains (Opperman et al., 2010), based on (1) hydrologic connectivity between the river and the floodplain, and between upstream and downstream sections; (2) hydrologic variability patterns and their links to local and regional processes; and (3) the spatial scale required to sustain floodplain-associated processes and benefits, like migratory fish biodiversity. Our proposed framework provides an explicit quantification of the non-linear or direct response relationship of those considerations to hydropower expansion. Changes in connectivity, hydrologic variability patterns, and the spatial scale of processes result from a wide range of scenarios that produce equivalent levels of energy generation capacity. This finding underscores the advantage of system-level integrated approaches to hydropower planning and development as well as potential to minimize impacts without sacrificing generating capacity (Hartmann et al., 2013; Opperman et al., 2015), and demonstrates how consideration of the trade-offs between impacts and benefits can serve as a basis for a preventive approach. Another important finding of this research is related to how to design and evaluate guiding principles that can be transparent and adopted by policy makers and project developers; our case study illustrates some examples of the adoption of rules that take advantage of the non-linearity of impacts on freshwater systems, and explores how to inform decision makers through simple rules that can enable conditions that avoid or reduce impacts on basin-level key processes.

Likewise, a relevant contribution is the enhancements to the WEAP modeling platform to resolve water balance dynamics of floodplains and wetlands. Our study shows that the hydrologic dynamics of water storage in floodplains on a monthly to decadal scale can be represented with these enhancements. In the case of the MRB, this enables WEAP to successfully resolve the lowland floodplains water balance at medium scales (~1000 to 10 000 km^2), while linking the simulation of these dynamics to upstream water management practices. By providing an improved understanding of the linkages between climate variability, system operation, and floodplain dynamics, this modelling approach can contribute in the consideration of floodplains dynamics into water management infrastructure development and operation decisions as well as in ecosystem conservation or restoration projects.

Colombia's regulatory framework—as other countries'—currently omits any consideration of basin-level impacts of hydropower expansion; the current study provides a method to include such considerations. The wide range of scenarios, from those producing outcomes with relatively small additional environmental impacts, to those that virtually eliminate basin-level processes, provides huge potential to avoid undesirable outcomes through a comprehensive integration of system-level performance metrics into hydropower planning. The challenge is integrating these considerations into policy design, which is currently highly reactionary and market driven.

5.2 Implication of the case study

The most recent analysis of sediment yield changes, performed with records from 1972 to 2010, shows no significant trend in observed sediment loads at the mouth of the Magdalena River (Restrepo et al., 2015). However, our study estimated sediment reduction due to reservoir trapping in 1977 and 2010 at 5.3 and 18.4%, respectively, equivalent to an average decrease of 0.40% yr^{-1}. In addition to reservoir effects, sediment trapping must be discussed in relation to other controls on sediment yield and transport, in particular to the clearing of natural vegetation for land cultivation, which is likely to result in increased river sediment yields (Walling and Fang, 2003). Over the same period of the study of Restrepo et al. (2015), average rates of natural cover loss in the MRB were estimated at 1.4 to 1.9% yr^{-1} (Etter et al., 2006; Restrepo et al., 2006). While the sediment retention/release dynamics of the Mompós floodplains are not well understood, the apparent equilibrium in basin-level sediment transport might be the result of the wetlands acting to buffer the sediment balance—with sediment added from land cover change being balanced by increased retention in the wetlands and/or additional sediment trapped by reservoirs being balanced by increased sediment released from the wetlands.

Despite the uncertain contribution of the Mompós floodplains to the MRB sediment balance, we must note that the baseline condition—which includes projects with an expected completion in 2018—represents a significant increase in sediment trapping (from 18.4 to 39.9%) over the reference period (1972-2010) reported by Restrepo et al. (2015). Further observation of the sediment balance of the Mompós floodplain can provide more definitive evidence of project impacts. Such analysis is urgent and relevant because under certain conditions, sediment deficits could induce basin-scale system transformations, such as net subsidence of wetland and floodplain areas and a progressive transformation into permanent water bodies. The wide range of increased sediment retention in future scenarios must also be a consideration in the assessment of hydropower contributions to carbon budgets, as studies have indicated a relationship between reservoirs' retention of organic sediments and greenhouse gas emissions (Deemer et al., 2016; Maeck et al., 2013); sediment retention is also important to the operation and longevity of hydropower dams, from a system-level perspective.

Loss of longitudinal connectivity by dams has been reported as one of the major threats to fish in the MRB, especially for migratory species and commonly fished species (Carvajal-Quintero et al., 2017; López-Casas et al., 2016). Those findings are supported by the results presented here, with the highest values of river fragmentation (up to 97.3%) incurred by dams situated between 400 and 1500 masl (Figure 6). Loss of longitudinal connectivity through river fragmentation could be affecting more than the migratory species evaluated here; it is important to note that this elevation range (400 to 2000 masl)

contains the highest fish species richness in the MRB, including several endemic species distributed along the tributaries having the densest dam development (Carvajal-Quintero et al., 2015; Jaramillo-Villa et al., 2010). This study prioritized evaluation of the impacts of longitudinal loss, but dams and associated reservoirs also affect lateral (local) connectivity as well as vertical connectivity (connection to groundwater).

Additionally, and as illustrated, upstream hydrologic alteration can produce heterogeneous effects in the floodplain lowlands, but the most immediate consequences seem related to changes in the amplitude, magnitude, extension, and seasonal variation of floodplain inundation and wetland water storage in low- and extreme-low flow conditions (Figure 12). These, along with changes in sediment inputs due to discharge regulation in the Mompós Depression, can alter important environmental signals and stimuli for fish migration, from the floodplain to the upstream tributaries. Loss of sediment inputs—and consequently of nutrient inputs—to the floodplains, which form a nursery and feeding area for migratory fish, can affect available energy reserves for the migration and reproductive maturation essential for reproduction in the upstream tributaries, as discussed by López-Casas et al. (2016). There are other important biological effects which should be evaluated in relation to changes in the composition and functional structure of the floodplain fish assemblages in the Mompós Depression. These changes have been documented in other basins, such as the Amazon (Röpke et al., 2017). Hydrologic alteration in combination with over-fishing and habitat conversion in the lowland floodplain in the Mompós Depression could profoundly affect the food security of the people that live in the lower MRB and depend on fisheries for their food supply and income.

Our findings also reveal a distinct response of the Mompós Depression floodplains based on the relative locations of dams in the basin. Under current conditions, this system seems more sensitive to artificial regulation in the Magdalena River than in the Cauca. Hydropower in the Cauca River seems to have little additional effect in terms of alteration of floodplain inundation dynamics, as significant loss of connectivity four decades ago continues to affect marshes on the west bank (the Ayapel and San Marcos). Additionally, the reservoirs of the Cauca have little influence over regulation of extreme events. This result, however, should be viewed in light of some proposals to replace the current levee on the west back of the Cauca with infrastructure that could restore the hydraulic connection between these systems. The WEAP model developed in this study can contribute to the evaluation of such measures.

6 Conclusion

This paper presents a framework to quantify impacts and trade-offs to inform hydropower expansion decisions, thus enabling an integrated approach of basin-level physical, environmental, and ecosystem processes. Following Opperman et al. (2010), we focused on functional lowland floodplain systems as key basin-level environmental features, considering the impacts of hydropower expansion on (1) hydrologic connectivity between the river and the floodplain, and between upstream and downstream sections; (2) hydrologic variability patterns and their links to local and regional processes; and (3) the spatial scale required to sustain floodplain-associated processes and benefits, like migratory fish biodiversity. Our analysis illustrates the non-linear behavior of cumulative impacts, characterized by a wide range of potential outcomes for equivalent

energy expansion configurations, and demonstrates a practical approach to inform decision makers on how to design effective guidelines to effectively protect—or avoid additional impacts on—key basin-scale processes and ecosystems.

As part of this study we developed a set of enhancements to WEAP that allow for simulation of water balance dynamics of floodplains and wetlands. By providing an improved understanding of the linkages between climate variability, system operation, and floodplain dynamics, these new routines can guide the implementation of water management infrastructure development as well as ecosystem conservation or restoration projects. Both components are critical to the sustainable development of Colombia and many other countries.

From a planning perspective, we compared possible scenarios of hydropower development (as combinations of projects) in order to meet expected national expansion goals for 2050. In the case of the MRB, our analysis shows that baseline hydropower conditions have already significantly altered multiple basin-level processes vital to the health of the Mompós wetlands floodplains, in particular loss of longitudinal connectivity of spawning habitats of migratory fish (-54.8%) and decreased sediment transport (-39%), while flow regime and wetland dynamics maintain near natural conditions. Development scenarios, however, show a potential range up to one order of magnitude of additional impacts across comparable hydropower capacity. Some future development scenarios can result in significant physical or hydrologic alteration, i.e. a loss of longitudinal connectivity to virtually all remaining spawning habitat for migratory fish and significant reductions of sediment loads, while substantially altering floodplain (lateral) seasonal inundation dynamics in extensive areas of the Mompós Depression. Our analysis of possible scenarios, however, indicates that other scenarios would result in much lower differential changes. This emphasizes the need for comprehensive basin-level approaches to water infrastructure planning that integrate broader environmental and cumulative impacts to achieve balanced outcomes across a wide range of objectives.

We recognize that the metrics used in this analysis, while selected to provide an objective insight into multiple basin-scale key processes, are still proxies with no direct representation of the specific ecological processes of the MRB. Nevertheless, the proposed framework can serve as a basis to guide detailed studies at the reach scale to establish direct relationships.

Acknowledgements

This work was supported by USAID Cooperative Agreement Award No. AID-S14-A-13-00004 and AID-514-A-12-00002, the Rio Magdalena Watershed Management Program, and “Generación del Bicentenario” scholarship program funded by Colombia’s *Departamento administrativo de ciencia, tecnología e innovación* - Colciencias. The authors would like to thank A. Hereford for her contributions in writing assistance, technical editing, language editing, and proofreading.

References

Angarita, H., Delgado, J., Escobar-Arias, M. I. and Walschburger, T.: Escenarios de alteración regional del regimen hidrológico en la cuenca Magdalena-Cauca por intensificación de la demanda para hidroenergía, in Memorias del Congreso Internacional AGUA, Universidad del Valle, Cali, Colombia, 2013.

ARCADIS Nederland BV and JESYCA S.A.S.: Plan Maestro Fluvial de Colombia 2015, Prepared for Ministerio de Transporte and Departamento Nacional de Planeación Bogotá, Colombia, 2015.

Arias, M. E., Piman, T., Lauri, H., Cochrane, T. A. and Kummu, M.: Dams on Mekong tributaries as significant contributors of hydrological alterations to the Tonle Sap Floodplain in Cambodia, Hydrol. Earth Syst. Sci., 18(12), 5303–5315, doi:10.5194/hess-18-5303-2014, 2014.

Bayley, P. B.: Understanding Large River–Floodplain Ecosystems, Bioscience, 45(3), 1995.

Carvajal-Quintero, J. D., Escobar, F., Alvarado, F., Villa-Navarro, F. A., Jaramillo-Villa, Ú. and Maldonado-Ocampo, J. A.: Variation in freshwater fish assemblages along a regional elevation gradient in the northern Andes, Colombia, Ecol. Evol., 5(13), 2608–2620, doi:10.1002/ece3.1539, 2015.

Carvajal-Quintero, J. D., Januchowski-Hartley, S. R., Maldonado-Ocampo, J. A., Jézéquel, C., Delgado, J. and Tedesco, P. A.: Damming Fragments Species Ranges and Heightens Extinction Risk, Conserv. Lett., 0(0), 1–9, doi:10.1111/conl.12336, 2017.

Cramton, P. and Stoft, S.: Colombia Firm Energy Market, in Proceedings of the 40th Annual Hawaii International Conference on System Sciences, HICSS., Waikoloa, Hawaii, USA., 2007.

Dang, T. D., Cochrane, T. A., Arias, M. E., Van, P. D. T. and de Vries, T.: Hydrological alterations from water infrastructure development in the Mekong floodplains, Hydrol. Process., doi:10.1002/hyp.10894, 2016.

Deemer, B. R., Harrison, J. A., Li, S., Beaulieu, J. J., Delsontro, T., Barros, N., Bezerra-Neto, J. F., Powers, S. M., Dos Santos, M. A. and Vonk, J. A.: Greenhouse gas emissions from reservoir water surfaces: A new global synthesis, Bioscience, 66(11), 949–964, doi:10.1093/biosci/biw117, 2016.

Dendy, F. E.: Sediment trap efficiency of small reservoirs, Trans. ASAE, 17(5), 898–908, doi:10.13031/2013.36994, 1974.

Departamento Nacional de Planeación: Estudio del Sector de Energía Eléctrica - Inventario de recursos hidroenergéticos, Bogotá, Colombia, 1979.

DePhilip, M. and Moberg, T.: Ecosystem flow recommendations for the Upper Ohio River Basin in Western Pennsylvania, Harrisburg, PA, 2013.

DHI: MIKE21, [Software], DHI Water & Environment Pty Ltd., https://www.mikepoweredbydhi.com/products/mike-21, 2016.

Dutta, D., Teng, J., Vaze, J., Lerat, J., Hughes, J. and Marvanek, S.: Storage-based approaches to build floodplain inundation modelling capability in river system models for water resources planning and accounting, J. Hydrol., 504, 12–28, doi:10.1016/j.jhydrol.2013.09.033, 2013.

Dynesius, M. and Nilsson, C.: Fragmentation and Flow Regulation of River Systems in the Northern Third of the World, Science, 266(5186), 753–762, doi:10.1126/science.266.5186.753, 1994.

Etter, A., McAlpine, C., Wilson, K., Phinn, S. and Possingham, H.: Regional patterns of agricultural land use and deforestation in Colombia, Agric. Ecosyst. Environ., 114(2–4), 369–386, doi:10.1016/j.agee.2005.11.013, 2006.

FAO: Colombia: Pesca en Cifras/2014, Food and Agriculture Organization of the United Nations, Bogotá, Colombia, http://aunap.gov.co/wp-content/uploads/2016/05/Pesca_en_cifras.pdf, 2015.

Fausch, K. D., Torgersen, C. E., Baxter, C. V and Li, H. W.: Landscapes to Riverscapes : Bridging the Gap between Research and Conservation of Stream Fishes, Bioscience, 52(6), 483–498, 2002.

Fitzhugh, T. W. and Vogel, R. M.: The impact of dams on flood flows in the United States, River Res. Appl., 27(10), 1192–1215, doi:10.1002/rra.1417, 2011.

Fullerton, A. H., Burnett, K. M., Steel, E. A., Flitcroft, R. L., Pess, G. R., Feist, B. E., Torgersen, C. E., Miller, D. J. and Sanderson, B. L.: Hydrological connectivity for riverine fish: Measurement challenges and research opportunities, Freshw. Biol., 55(11), 2215–2237, doi:10.1111/j.1365-2427.2010.02448.x, 2010.

Galvis, G. and Mojica, J. I.: The Magdalena River fresh water fishes and fisheries, Aquat. Ecosyst. Health Manag., 10(2), 127–139, doi:10.1080/14634980701357640, 2007.

Gao, Y., Vogel, R. M., Kroll, C. N., Poff, N. L. and Olden, J. D.: Development of representative indicators of hydrologic alteration, J. Hydrol., 374(1–2), 136–147, doi:10.1016/j.jhydrol.2009.06.009, 2009.

Grant, G. E., Schmidt, J. C. and Lewis, S. L.: A Geological Framework for Interpreting Downstream Effects of Dams on Rivers, in A Peculiar River, edited by J. E. O'Connor and G. E. Grant, pp. 209–225, American Geophysical Union, 2003.

Grill, G., Lehner, B., Lumsdon, A. E., MacDonald, G. K., Zarfl, C. and Reidy Liermann, C.: An index-based framework for assessing patterns and trends in river fragmentation and flow regulation by global dams at multiple scales, Environ. Res. Lett., 10(1), 15001, doi:10.1088/1748-9326/10/1/015001, 2015.

Hartmann, J., Harrison, D., Opperman, J. J. and Gill, R.: The Next Frontier of Hydropower Sustainability: Planning at the System Scale, 2013.

IDEAM: Sistemas morfogénicos del territorio colombiano, Instituto de Hidrología, Meteorología y Estudios Ambientales, Bogotá, Colombia, http://documentacion.ideam.gov.co/openbiblio/bvirtual/021769/Sistemas_morf_Territ_Col_Ideam_Contenido.pdf, 2010.

IDEAM: Estudio Nacional del Agua, Instituto de Hidrología, Meteorología y Estudios Ambientales, Bogotá, Colombia, http://documentacion.ideam.gov.co/openbiblio/bvirtual/023080/ENA_2014.pdf, 2014.

IDEAM, IGAC, IAvH, Invemar, ISinchi and IIAP: Ecosistemas continentales, costeros y marinos de Colombia, Instituto de Hidrología, Meteorología y Estudios Ambientales, Bogotá, Colombia, 2007.

Jaramillo-Villa, Ú., Maldonado-Ocampo, J. A. and Escobar, F.: Altitudinal variation in fish assemblage diversity in streams of the central Andes of Colombia, J. Fish Biol., 76(10), 2401–2417, doi:10.1111/j.1095-8649.2010.02629.x, 2010.

Jaramillo, U., Cortés-Duque, J. and Flórez, C., Eds.: Colombia Anfibia. Un país de humedales. Volumen 1., Instituto de Investigación de Recursos Biológicos Alexander von Humboldt, Bogotá, Colombia, 2015.

Jiménez-Segura, L. F., Restrepo-Santamaría, D., López-Casas, S., Delgado, J., Valderrama, M., Álvarez, J. and Gómez, D.: Ictiofauna y desarrollo del sector hidroeléctrico en la cuenca del río Magdalena-Cauca, Colombia, Biota Colomb., 15(2), www.humboldt.org.co/biota, 2014.

Jimenez, M.: Cuentas de sedimentos a escala de cuencas usando conceptualizaciones de modelos conocidos y confiables, y aplicación de información secundaria, Medellín, Colombia, 2016.

Lasso, C. A., Gutiérrez, F. de P., Morales-Betancourt, M. A., Agudelo, E., Ramírez-Gil, H. R. and Ajiaco-Martínez, R. E., Eds.: Pesquerías continentales de Colombia: cuencas del Magdalena-Cauca, Sinú, Canalete, Atrato, Orinoco, Amazonas y vertiente del Pacífico. Serie Editorial Recursos Hidrobiológicos y Pesqueros Continentales de Colombia, Instituto de Investigación de los Recursos Biológicos Alexander von Humboldt, Bogotá, Colombia, 2011.

Lehner, B. and Grill, G.: Global river hydrography and network routing: baseline data and new approaches to study the world's large river systems, Hydrol. Process., 27(15), 2171–2186, available at www.hydrosheds.org, 2013.

Lehner, B., Verdin, K. and Jarvis, A.: New global hydrography derived from spaceborne elevation data, Eos, Trans. AGU, 89(10), 93–94, 2008.

Lewin, J. and Ashworth, P. J.: Defining large river channel patterns: Alluvial exchange and plurality, Geomorphology, 215, 83–98, doi:http://doi.org/10.1016/j.geomorph.2013.02.024, 2014.

Liu, C., White, M. and Newell, G.: Selecting thresholds for the prediction of species occurrence with presence-only data, J. Biogeogr., 40(4), 778–789, doi:10.1111/jbi.12058, 2013.

López-Casas, S., Jiménez-Segura, L. F. and Pérez-Gallego, C. M.: Peces migratorios al interior de una central hidroeléctrica: caso Miel I, cuenca del río Magdalena (Caldas-Antioquia), Colombia, Biota Colomb., 15(2), 2014.

López-Casas, S., Jiménez-Segura, L. F., Agostinho, A. A. and Pérez, C. M.: Potamodromous migrations in the Magdalena River basin: bimodal reproductive patterns in neotropical rivers, J. Fish Biol., 1–15, doi:10.1111/jfb.12941, 2016.

Maeck, A., DelSontro, T., McGinnis, D. F., Fischer, H., Flury, S., Schmidt, M., Fietzek, P. and Lorke, A.: Sediment Trapping by Dams Creates Methane Emission Hot Spots, Environ. Sci. Technol., 47(15), 8130–8137, doi:10.1021/es4003907, 2013.

Maldonado-Ocampo, J. A., Vari, R. and Usma, J.: Checklist of the freshwater fishes of Colombia, Biota Colomb., 9(2), 143–237, http://www.humboldt.org.co/biota/index.php/Biota/article/view/170 (Accessed 1 October 2013), 2008.

Moriasi, D. N., Arnold, J. G., Liew, M. W. Van, Bingner, R. L., Harmel, R. D. and Veith, T. L.: Model evaluation guidelines for systematic quantification of accuracy in watershed simulations, Trans. Am. Soc. Agric. Biol. Eng., 50(3), 885–900, 2007.

Opperman, J. J., Luster, R., McKenney, B. A., Roberts, M. and Meadows, A. W.: Ecologically Functional Floodplains: Connectivity, Flow Regime, and Scale, J. Am. Water Resour. Assoc., 46(2), 211–226, doi:10.1111/j.1752-1688.2010.00426.x, 2010.

Opperman, J. J., Grill, G. and Hartmann, J.: The Power of Rivers: Finding balance between energy and conservation in hydropower development, Washington, D.C., http://www.nature.org/media/freshwater/power-of-rivers-report.pdf, 2015.

Pareja-Carmona, M. I. and Ospina-Pabón, J. G.: Listado taxonómico de especies ícticas de importancia pesquera en tres embalses del Oriente antioqueño, cuenca del río Magdalena, Colombia, Biota Colomb., 15(2), 2014.

Phillips, S. J., Dudík, M., Elith, J., Graham, C. H., Lehmann, A., Leathwick, J. and Ferrier, S.: Sample selection bias and presence-only distribution models: Implications for background and pseudo-absence data, Ecol. Appl., 19(1), 181–197, doi:10.1890/07-2153.1, 2009.

Piman, T., Cochrane, T. A. and Arias, M. E.: Effect of proposed large dams on water flows and hydropower production in the Sekong, Sesan and Srepok rivers of the Mekong Basin, River Res. Appl., 22, 1085–1095, doi:10.1002/rra, 2016.

Poff, N. L. and Zimmerman, J. K. H.: Ecological responses to altered flow regimes: a literature review to inform the science and management of environmental flows, Freshw. Biol., 55(1), 194–205, doi:10.1111/j.1365-2427.2009.02272.x, 2010.

Poff, N. L., Allan, J. D., Bain, M. B., Karr, J. R., Pretegaard, K. L., Richter, B. D., Sparks, R. E. and Stromberg, J. C.: The natural flow regime, Bioscience, 47(11), 1997.

Posada G., L. and Rhenals, R. L.: Controles Fluviales del Río Cauca en la Región de La Mojana, in XVII Seminario Nacional de Hidráulica e Hidrología, pp. 655–662, Popayán, Colombia., 2006.

Poveda, G. and Mesa, O. J.: Feedbacks between hydrological processes in tropical South America and large-scale ocean–atmospheric phenomena, J. Clim., 10(10), 2690–2702, doi:10.1175/1520-0442(1997)010<2690:FBHPIT>2.0.CO;2, 1997.

Poveda, G., Jaramillo, A., Gil, M. M., Quiceno, N. and Mantilla, R. I.: Seasonality in ENSO-related precipitation, river discharges, soil moisture, and vegetation index in Colombia, Water Resour. Res., 37(8), 2169–2178, doi:10.1029/2000WR900395, 2001.

Poveda, G., Álvarez, D. M. and Rueda, Ó. A.: Hydro-climatic variability over the Andes of Colombia associated with ENSO: a review of climatic processes and their impact on one of the Earth's most important biodiversity hotspots, Clim. Dyn., 36(11–12), 2233–2249, doi:10.1007/s00382-010-0931-y, 2011.

Restrepo, J. C., Ortíz, J. C., Otero, L. and Ospino, S. R.: Transporte de sedimentos en suspensión en los principales ríos del Caribe colombiano: magnitud, tendencias y variabilidad, Rev. la Acad. Colomb. Ciencias Exactas, Físicas y Nat., 39(153), 527, doi:10.18257/raccefyn.209, 2015.

Restrepo, J. D., Kjerfve, B., Hermelin, M. and Restrepo, J. C.: Factors controlling sediment yield in a major South American drainage basin: the Magdalena River, Colombia, J. Hydrol., 316(1–4), 213–232, doi:10.1016/j.jhydrol.2005.05.002, 2006.

Richter, B. D., Baumgartner, J. V., Powell, J. and Braun, D. P.: A Method for Assessing Hydrologic Alteration within Ecosystems, Conserv. Biol., 10(4), 1163–1174, doi:10.1046/j.1523-1739.1996.10041163.x, 1996.

Richter, B. D., Baumgartner, J. V., Braun, D. P. and Powell, J.: A spatial assessment of hydrologic alteration within a river network, Regul. Rivers Res. Manag., 14, 329–340, ftp://ftp.sratx.org/pub/BBEST/Library/BBEST_025-AssessmentHydologicAlterationRiverNetwork.pdf (Accessed 17 September 2013), 1998.

Ritter, J.: Optimisation of hydropower dam cascade operations with respect to energy generation, flood hazard and flow regime alteration, using operational modelling: a case study in the Nechí catchment, Colombia, UNESCO-IHE, 2016.

Roberts, S.: ANUGA Open Source Hydrodynamic / Hydraulic Modelling Project, http://anuga.anu.edu.au/, 2017.

Röpke, C. P., Amadio, S., Zuanon, J., Ferreira, E. J. G., de Deus, C. P., Pires, T. H. S. and Winemiller, K. O.: Simultaneous abrupt shifts in hydrology and fish assemblage structure in a floodplain lake in the central Amazon, Sci. Rep., 7, doi:10.1038/srep40170, 2017.

Sanchez-Lozano, J., Ardila, F., Oliveros, J. J., Ramirez, W. D., Cardona, C. A., Garay, C. I., Verschelling, E., Becker, A. and Zagonjoll, M.: Hydraulic Modeling of Magdalena River Using SOBEK, in E-proceedings of the 36th IAHR world congress, pp. 1–13, The Hague, the Netherlands., 2015.

SEI: Water Evaluation and Planning - WEAP, [Software], Stockholm Environment Institute, 2017.

Smith, D. G.: Anastomosing river deposits, sedimentation rates and basin subsidence, Magdalena River, northwestern Colombia, South America, Sediment. Geol., 46, 177–196, 1986.

Strahler, A. N.: Quantitative analysis of watershed geomorphology, Trans. Am. Geophys. Union, 38(6), 913–920, doi:10.1029/TR038i006p00913, 1957.

Syvitski, J. P. M., Kettner, A. J., Overeem, I., Hutton, E. W. H., Hannon, M. T., Brakenridge, G. R., Day, J., Vörösmarty, C., Saito, Y., Giosan, L. and Nicholls, R. J.: Sinking deltas due to human activities, Nat. Geosci., 2(10), 681–686, 2009.

Tanner, W. F.: The incomplete flood plain: Reply, Geology, 2(6), 281, doi:10.1130/0091-7613(1974)2<281a:TIFPR>2.0.CO;2, 1974.

Tockner, K. and Stanford, J. A.: Riverine flood plains: present state and future trends, Environ. Conserv., 29(3), 308–330, doi:10.1017/S037689290200022X, 2002.

UPME: Plan de Expansión de Referencia Generación – Transmisión 2012-2025, Unidad de Planeación Minero Energética, Bogotá, Colombia, http://www1.upme.gov.co/index.php/servicios-de-informacion/noticias-del-sector/676.html, 2012.

UPME: Plan Energético Nacional, Unidad de Planeación Minero Energética, Bogotá, Colombia, http://www.upme.gov.co/docs/pen/pen_idearioenergetico2050.pdf, 2015.

USACE and RMA: HEC-RAS, [Software], http://www.hec.usace.army.mil/software/hec-ras/, US Army Corps of Engineers and Resource Management Associates, 2016.

Verdin, K. L. and Verdin, J. P.: A topological system for delineation and codification of the Earth's river basins, J. Hydrol., 218(1–2), 1–12, 1999.

Villa-Navarro, F. A., García-Melo, L. J., Zúñiga-Upegui, P., García-Melo, J. E., Quiñones-Montiel, J. M., Albornoz, J. G., Conde-Saldaña, C. C., Reinoso-Flórez, G., Gualtero-Leal, D. M. and Ángel-Rojas, V. J.: Historia de vida del bagre Imparfinis usmai (Heptapteridae: Siluriformes) en el área de influencia del proyecto hidroeléctrico El Quimbo, alto río Magdalena, Colombia, Biota Colomb., 15(2), 2014.

Vogel, R. M., Sieber, J., Archfield, S. A., Smith, M. P., Apse, C. D. and Huber-Lee, A.: Relations among storage, yield, and instream flow, Water Resour. Res., 43(5), 1–12, doi:10.1029/2006WR005226, 2007.

Vörösmarty, C. J., Meybeck, M., Fekete, B., Sharma, K., Green, P. and Syvitski, J. P. M.: Anthropogenic sediment retention: Major global impact from registered river impoundments, Glob. Planet. Change, 39(1–2), 169–190, doi:10.1016/S0921-8181(03)00023-7, 2003.

Walling, D. E. and Fang, D.: Recent trends in the suspended sediment loads of the world's rivers, Glob. Planet. Change, 39(1–2), 111–126, doi:10.1016/S0921-8181(03)00020-1, 2003.

Wilkinson, S. N., Prosser, I. P., Rustomji, P. and Read, A. M.: Modelling and testing spatially distributed sediment budgets to relate erosion processes to sediment yields, Environ. Model. Softw., 24(4), 489–501, 2009.

Williams, G. P. and Wolman, M. G.: Downstream effects of dams on alluvial rivers, http://pubs.er.usgs.gov/publication/pp1286, 1984.

XM: Informe de Operación del SIN y Administración del Mercado - Generación del SIN, Medellín, Colombia, http://informesanuales.xm.com.co/2014/SitePages/operacion/Informe de Operación del SIN_2014.pdf, 2014.

Yang, X. and Lu, X. X.: Estimate of cumulative sediment trapping by multiple reservoirs in large river basins: An example of the Yangtze River basin, Geomorphology, 227(August), 49–59, doi:10.1016/j.geomorph.2014.01.014, 2014.

Yates, D., Sieber, J., Purkey, D. and Huber-Lee, A.: WEAP21–A Demand-, Priority-, and Preference-Driven Water Planning Model: Part 1: Model Characteristics, Int. Water Resour. Assoc., 30(4), 487–500, 2005a.

Yates, D., Sieber, J., Purkey, D. and Huber-Lee, A.: WEAP21 – A Demand- , Priority- , and Preference-Driven Water Planning Model Part 1 : Model Characteristics, IWRA, Water Int., 30(4), 487–500, 2005b.

Zarfl, C., Lumsdon, A. E., Berlekamp, J., Tydecks, L. and Tockner, K.: A global boom in hydropower dam construction, Aquat. Sci., 77(1), 161–170, doi:10.1007/s00027-014-0377-0, 2014.

Zedler, J. B. and Kercher, S.: Wetland Resources: Status, Trends, Ecosystem Services, and Restorability, Annu. Rev. Environ. Resour., 30(1), 39–74, doi:10.1146/annurev.energy.30.050504.144248, 2005.

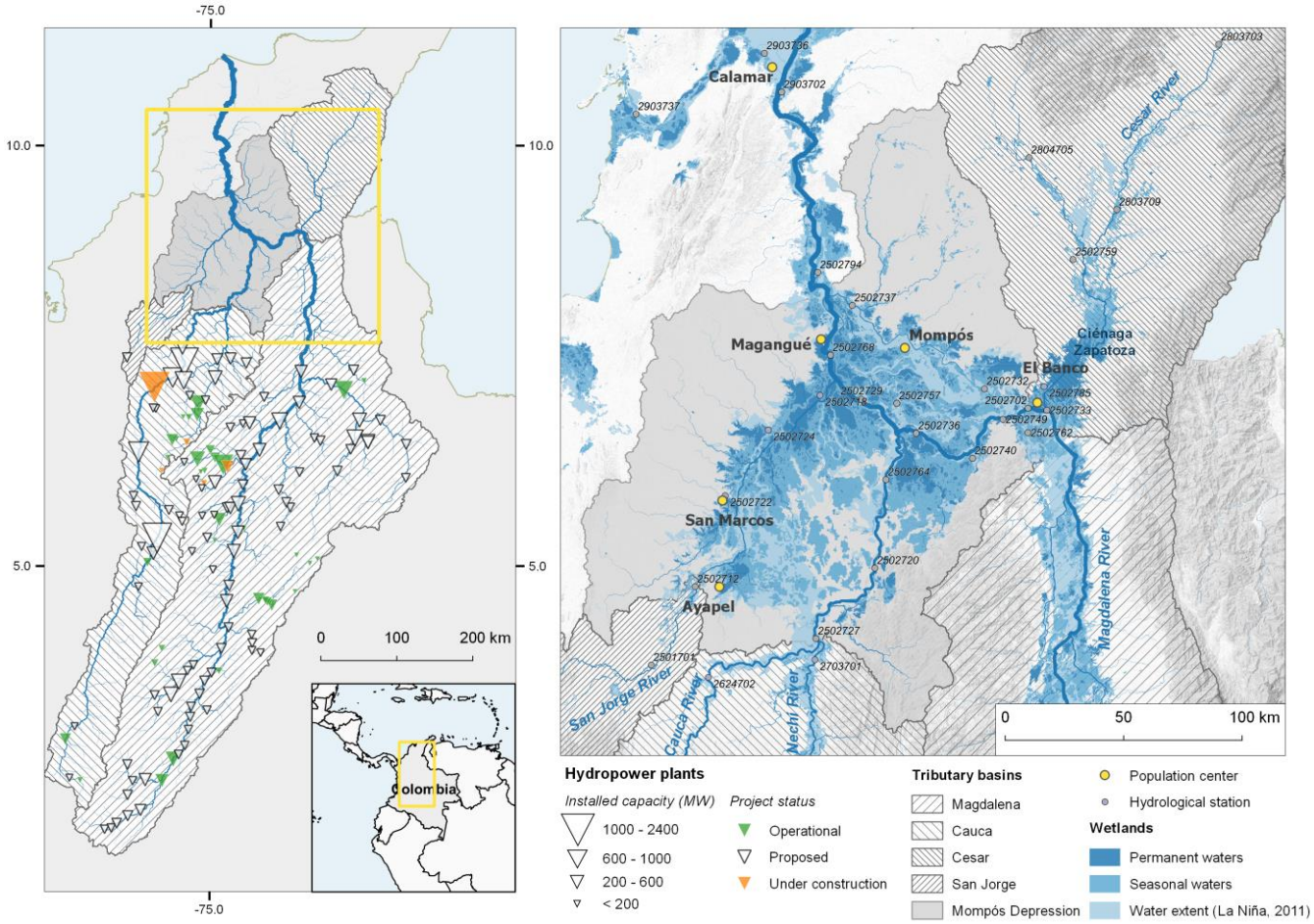

Figure 1. Map of the Magdalena River basin showing existing and proposed hydropower dams (Left), and the Mompós Depression low floodplains system and hydrological stations (numbered) referenced in the text (Right).

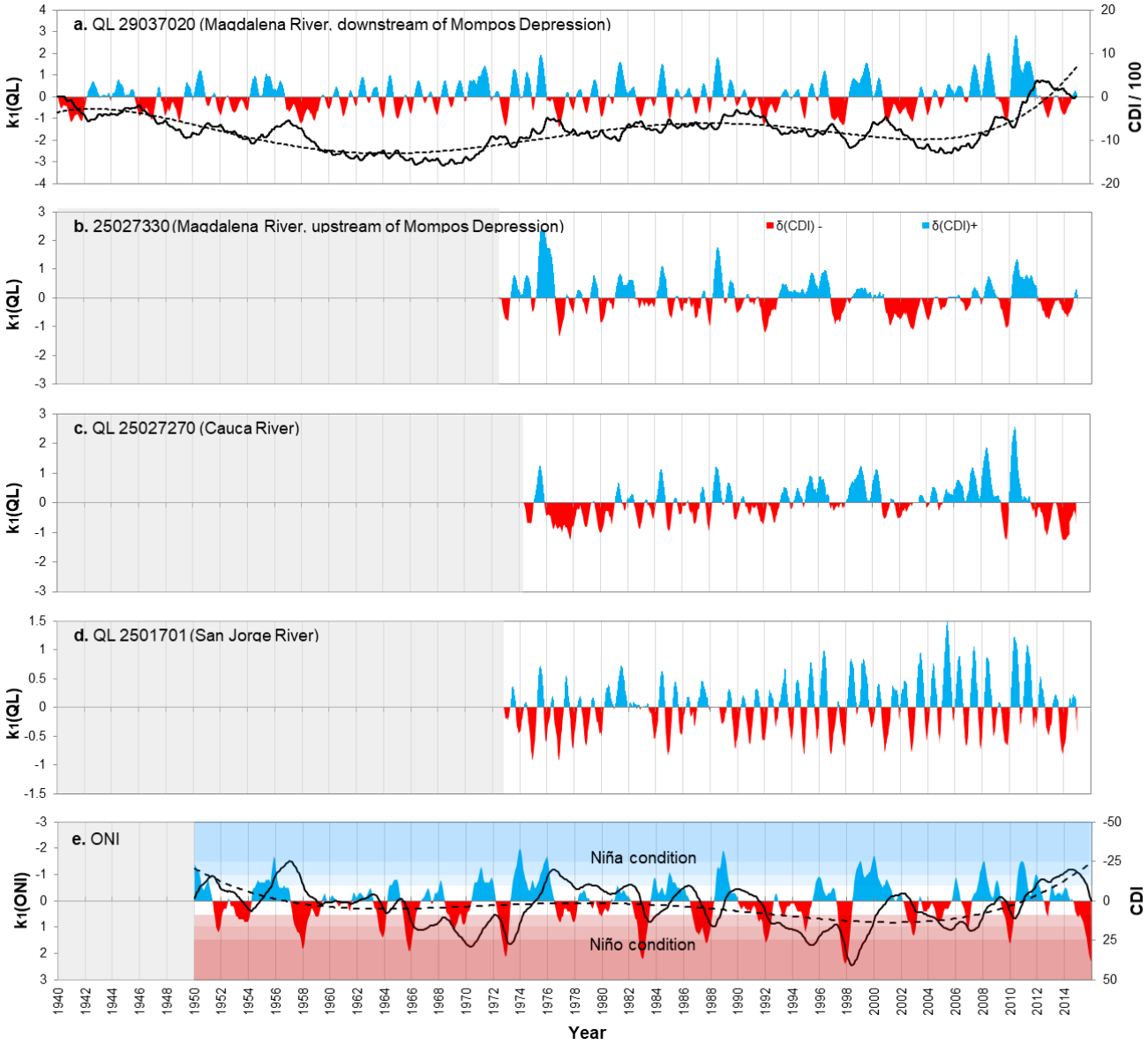

Figure 2. Streamflow inter-annual variability, expressed as the 6-month moving average of the k_1 anomaly (blue and red areas) and the corresponding cumulative anomaly (continuous black line) observed at streamflow (QL) gauges (graphs a-d) in comparison to the Oceanic Niño Index (ONI; graph e). Data gaps are shaded grey.

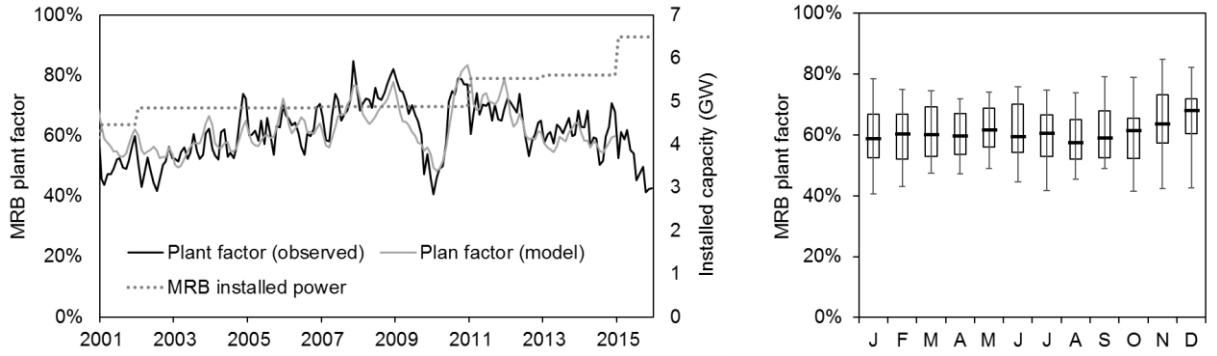

Figure 3. Aggregated observed and modeled plant factor of Magdalena River basin (MRB) hydropower plants (2001-2015), and seasonal variation of the plant factor over the observed period.

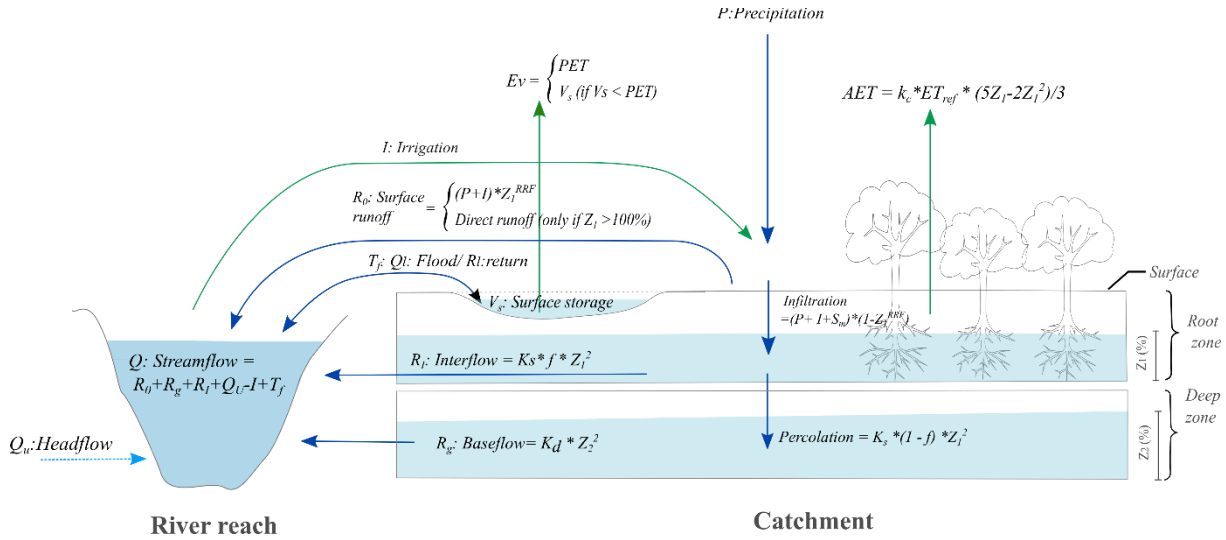

Figure 4. Schematic of the enhanced two-layer soil moisture model including a surface storage component.

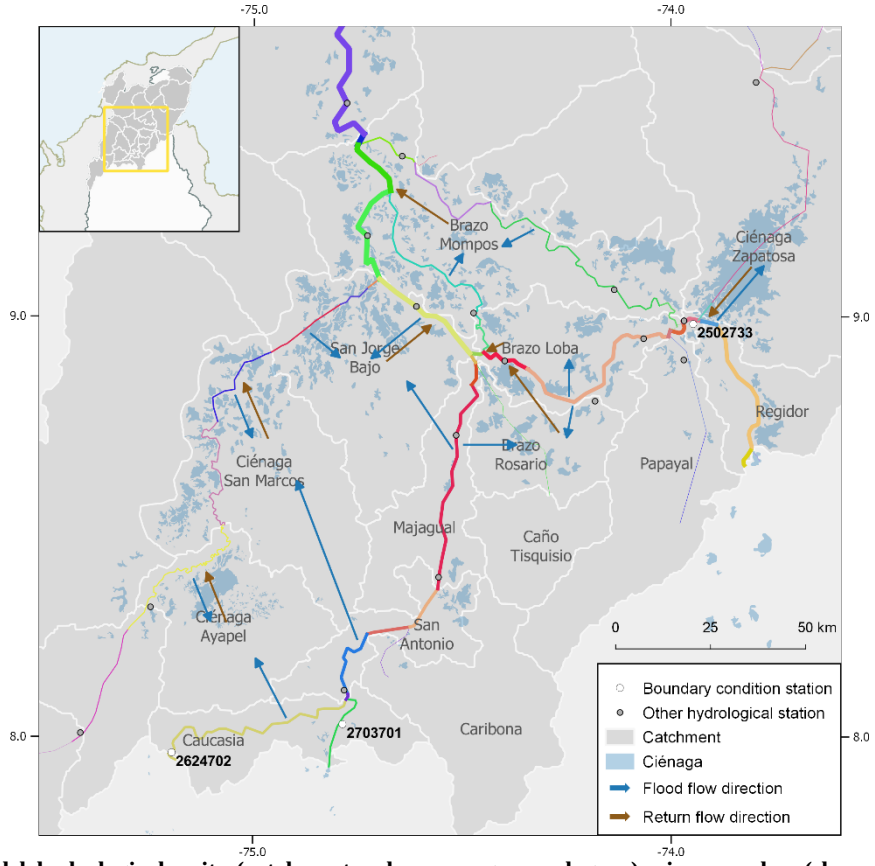

Figure 5. WEAP Model hydrological units (catchments, shown as grey polygons), river reaches (shown in different colors to illustrate the discretization of the fluvial network), and topological relationships between river reaches and wetland/floodplain areas (flood flows and returns). Stations corresponding to streamflow boundary conditions are labeled: 2502733 (Magdalena at Peñoncito), 2624702 (Cauca at La Coquera), and 2703701 (Nechí at La Esperanza).

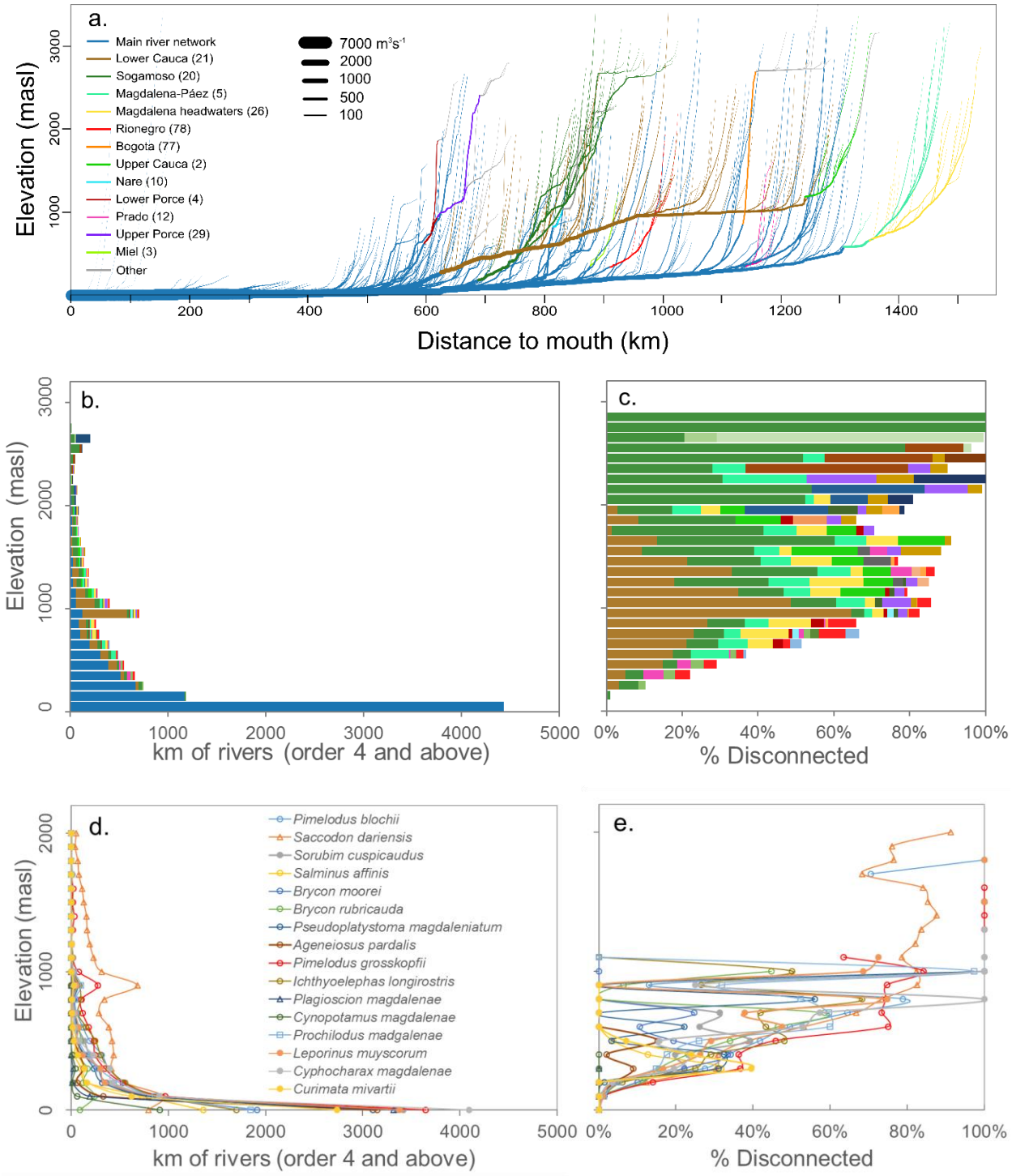

Figure 6. Baseline conditions of remaining river network connectivity by elevation (rivers of order 4 and above). Network fragments associated with specific barriers shown in different colors (a-c; Project IDs from Table 1). Habitat availability and loss by elevation ranges of migratory fish species (d, e).

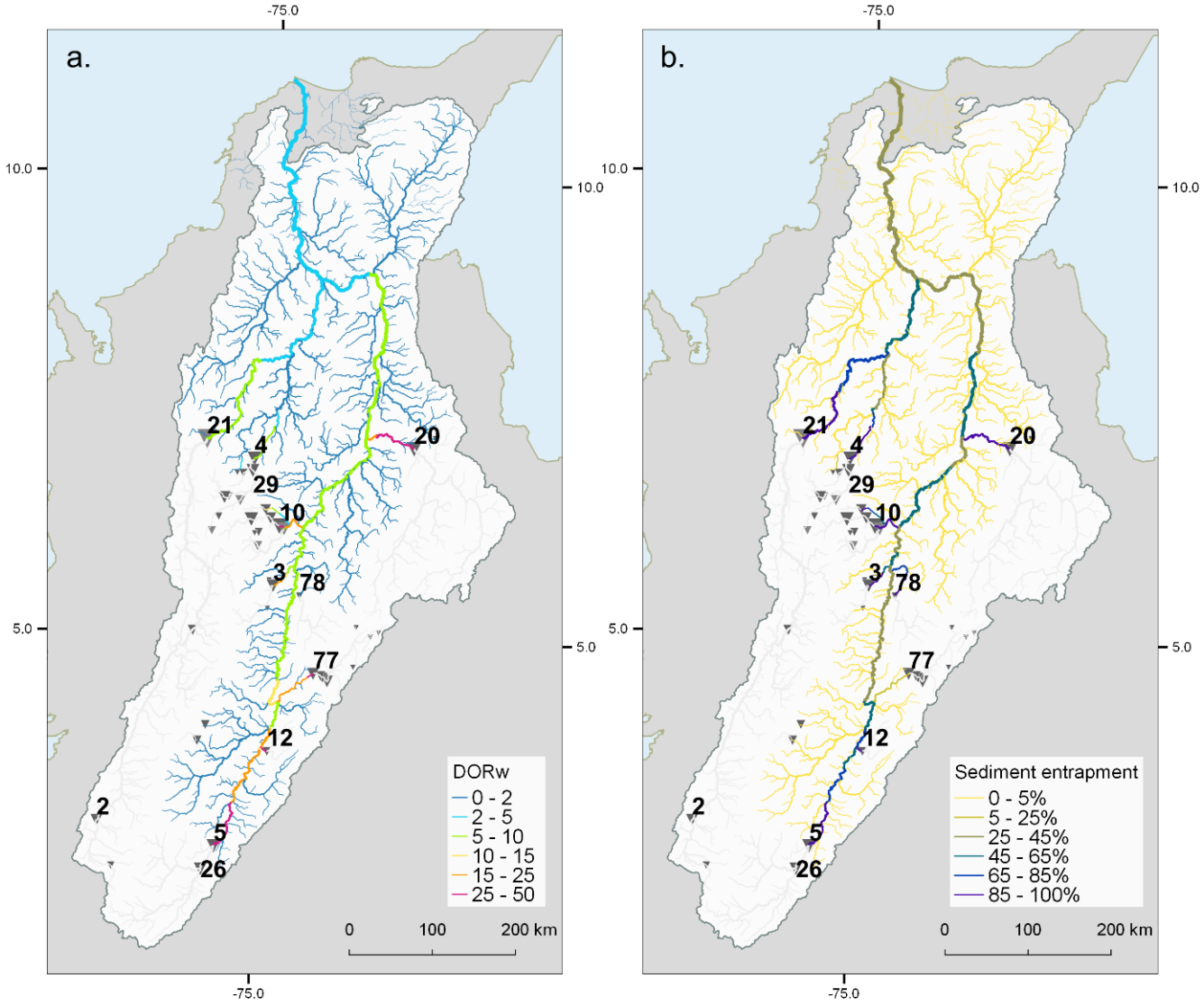

Figure 7. Baseline cumulative impacts of existing and under construction dams in the basin (symbolized by triangles): (Left) *DORw* weighted degree of regulation and (Right) percentage of sediment entrapment due to upstream reservoirs. Fragmented sections of river network are greyed out. Selected projects labeled with IDs used in Table 1.

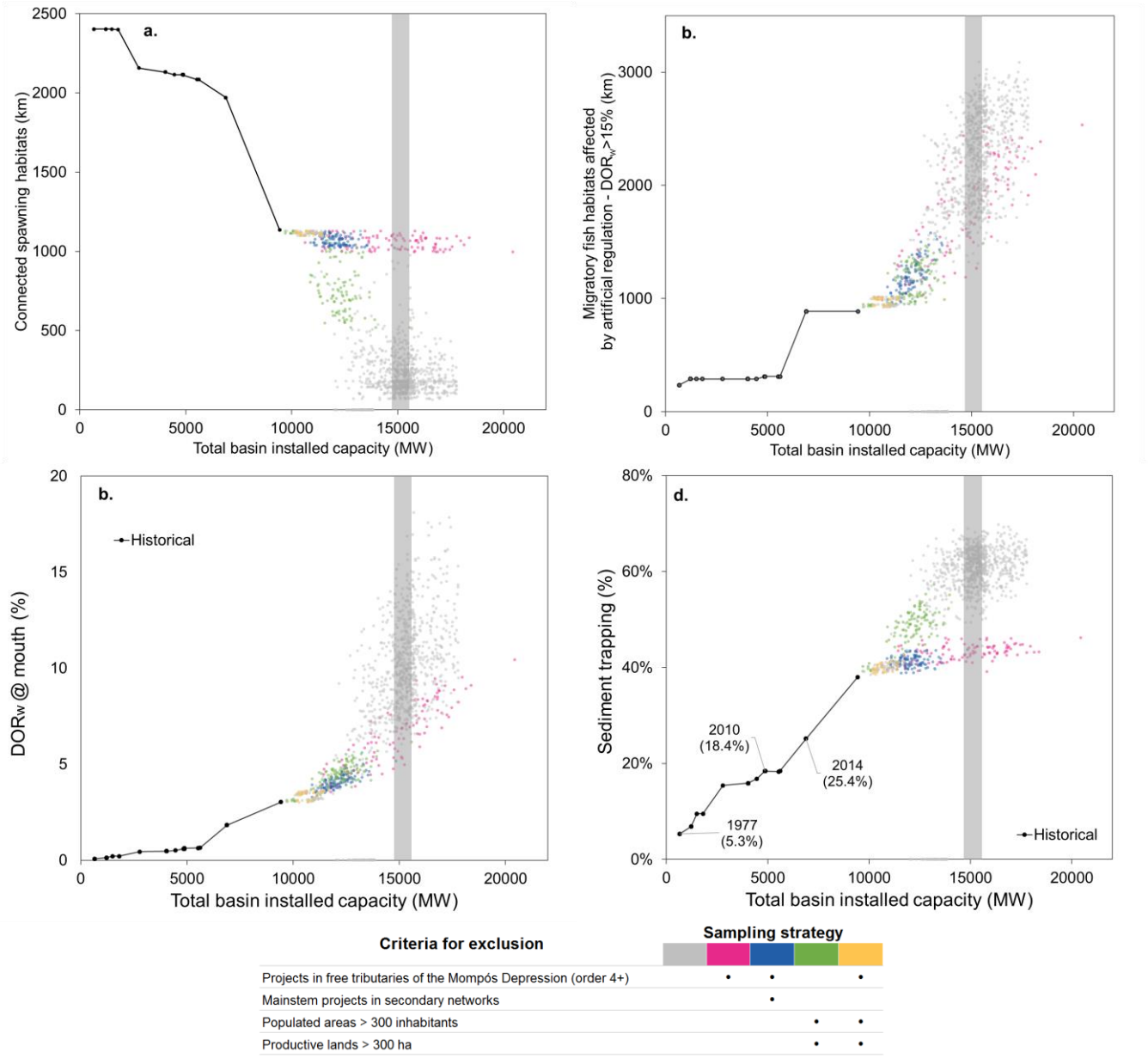

Figure 8. Indicators of basin-level cumulative alteration of historical hydropower development (lines) and randomly generated expansion scenarios (dots) using different sampling strategies (differentiated by color). Shaded area shows the range of expected capacity by 2050 (15 250±500 MW). a) Longitudinally connected river length at 0-400 masl (migration) and 400-1000 masl (spawning). b) Cumulative streamflow regulation measured as *weighted degree of regulation (DOR$_w$)*. c) Total sediment trapping in reservoirs upstream of the Mompós Depression. d) Percentage of basin runoff used for hydropower production.

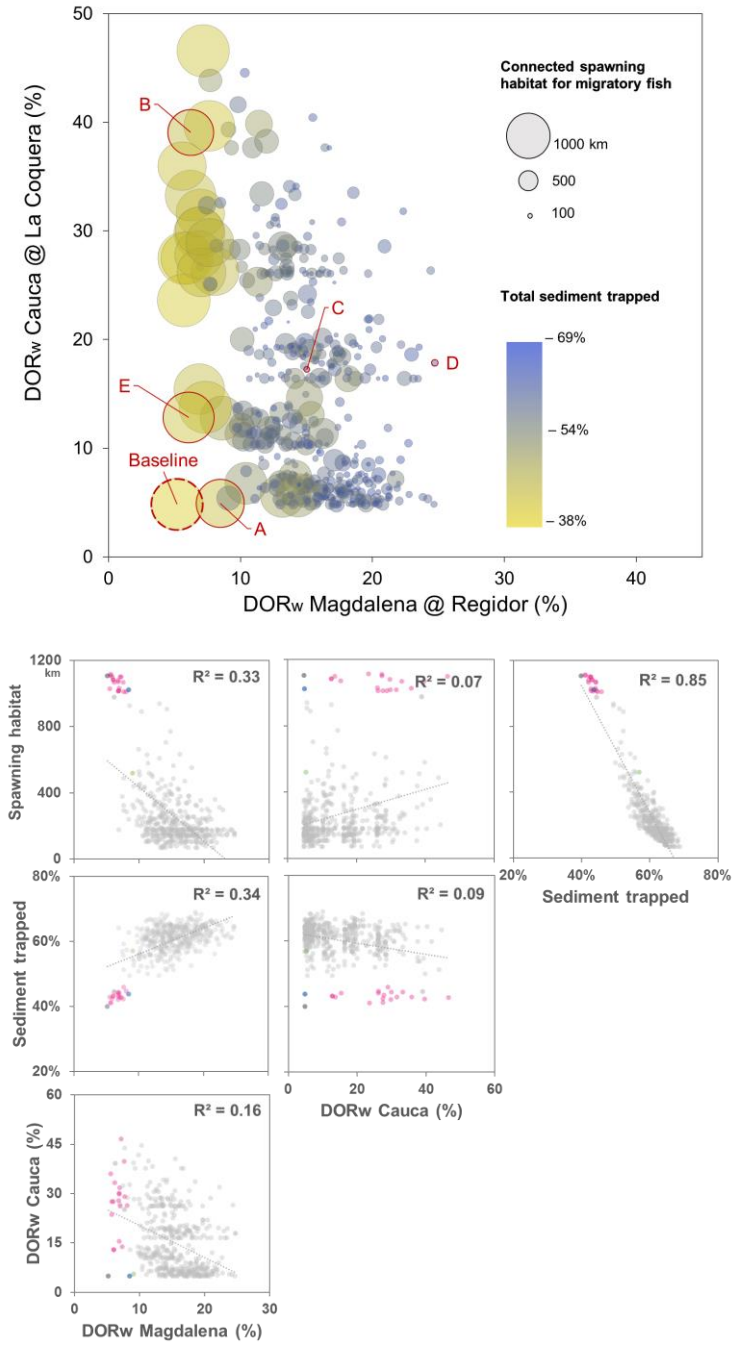

Figure 9. Trade-off plot for scenarios in the range of expected hydropower expansion (15 250±500MW). (Top): X and Y axes are expected DOR_w upstream of the Mompós Depression on the Magdalena and the Cauca, respectively; bubble size represents length of connected network in the range of 400-1000 masl (spawning habitat), and color indicates the expected loss of sediment load due to reservoir trapping. Selected scenarios for detailed analyses are labeled as A, B, C, D, and E. (Bottom) 2-D plots between individual metrics of basin-level impacts. Colors identify different sampling strategies following legend shown in Figure 8.

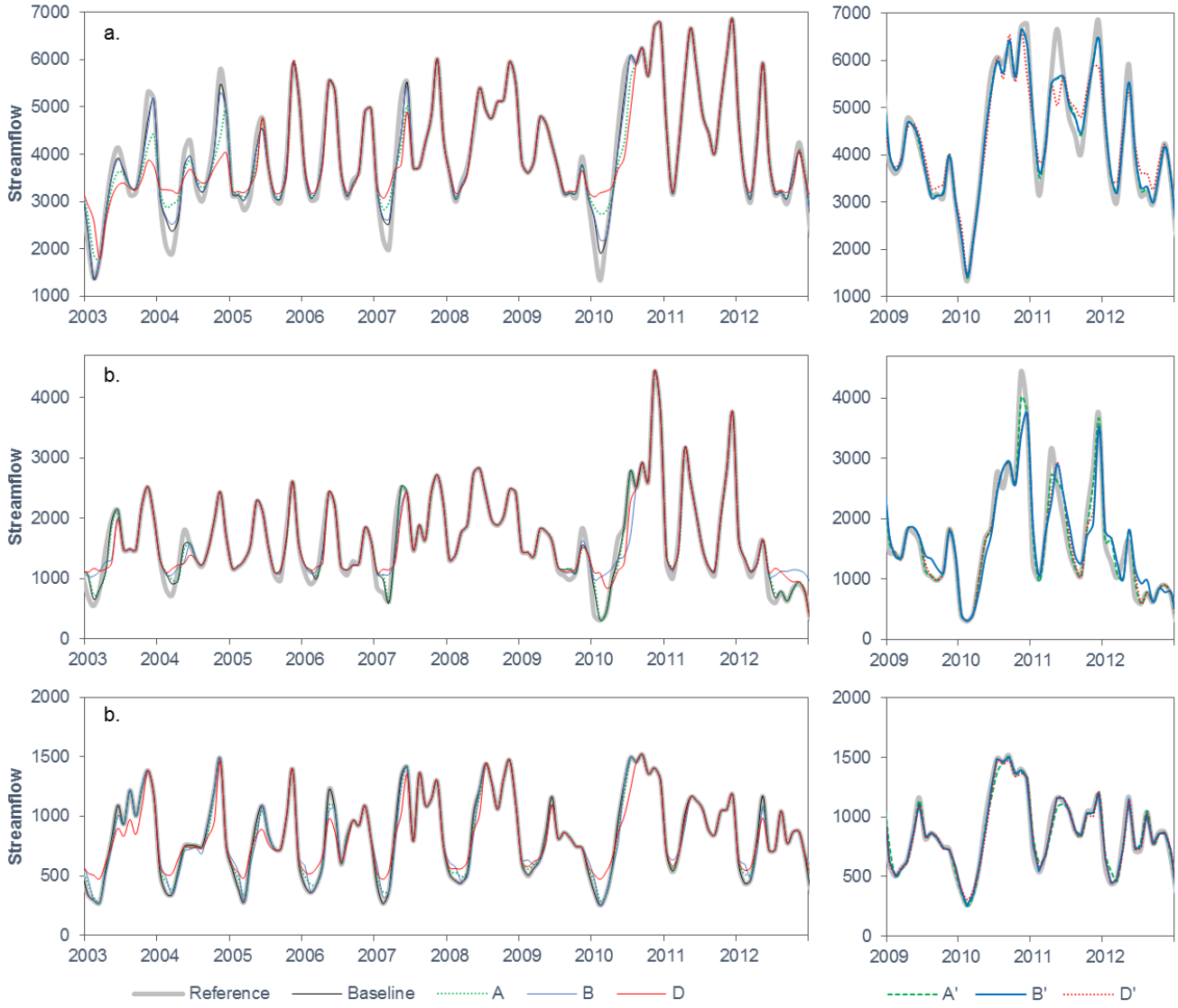

Figure 10. Comparison of 10-year sample (2003-2012) of simulated boundary conditions (monthly average streamflow) resulting from selected hydropower configurations A, B and D. Streamflow values are shown for stations on the a. Magdalena (2502733), b. Cauca (2624702), and c. Nechí (2703701) rivers, upstream of the Mompós Depression. Full period of boundary conditions is 1981-2013. Left plots show resulting simulation from scenarios from a hydropower priority operation. Right plots show examples of operation aiming to reduce flood peak magnitudes during the Niño-Niña 2009-2011 eventby maintaining low storage in reservoirs to regulate peak flows.

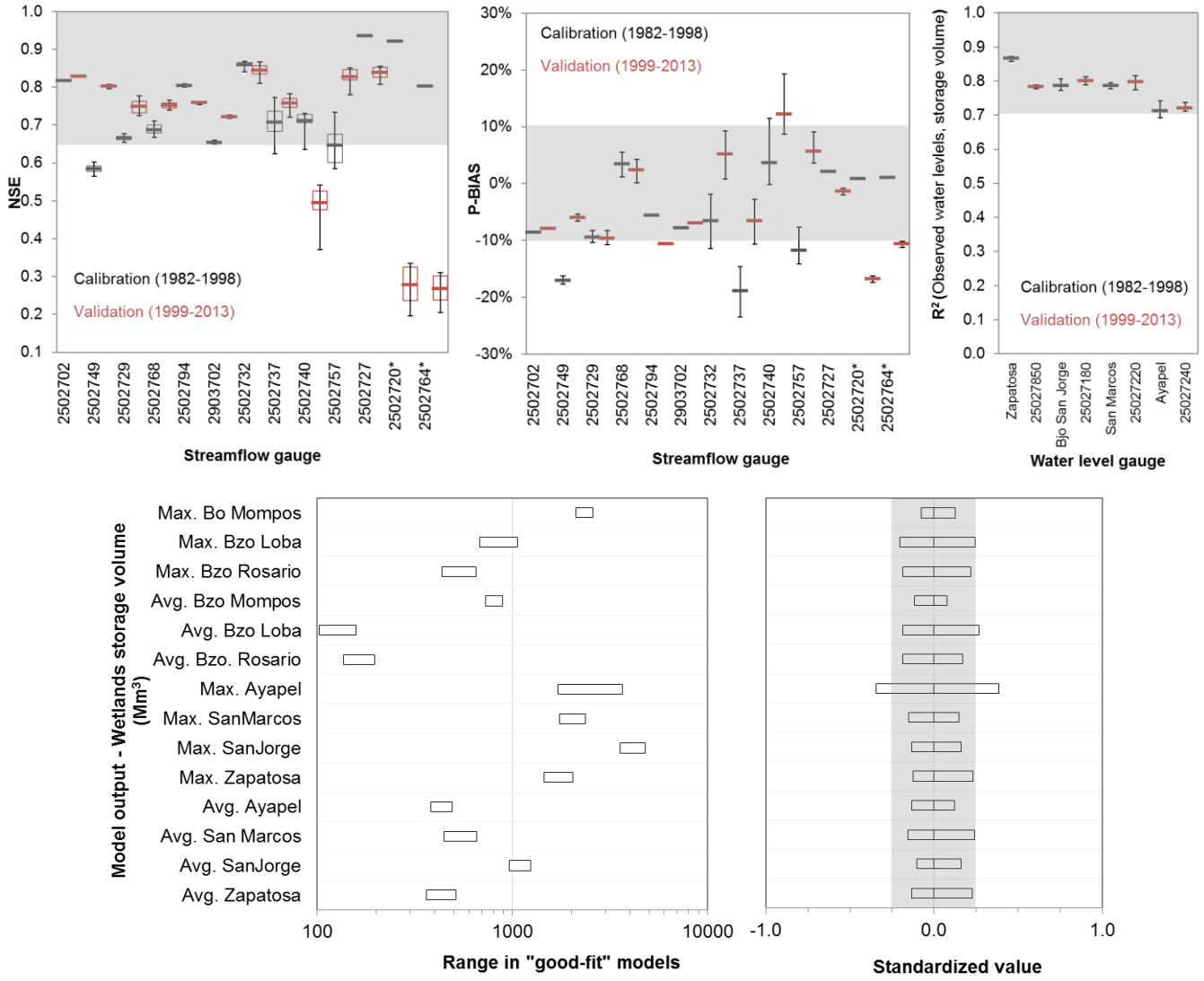

Figure 11. Comparison of the subset of models with highest performance obtained from Monte Carlo calibration: (Above) NSE and Percentile Bias of streamflow, and Correlation Coefficient of water levels and storage volumes. Acceptance ranges highlighted in grey. (Below) Model sensitivity of "good-fit models," in terms of average and maximum volume storage in the main floodplain sub-units of the Mompós Depression.

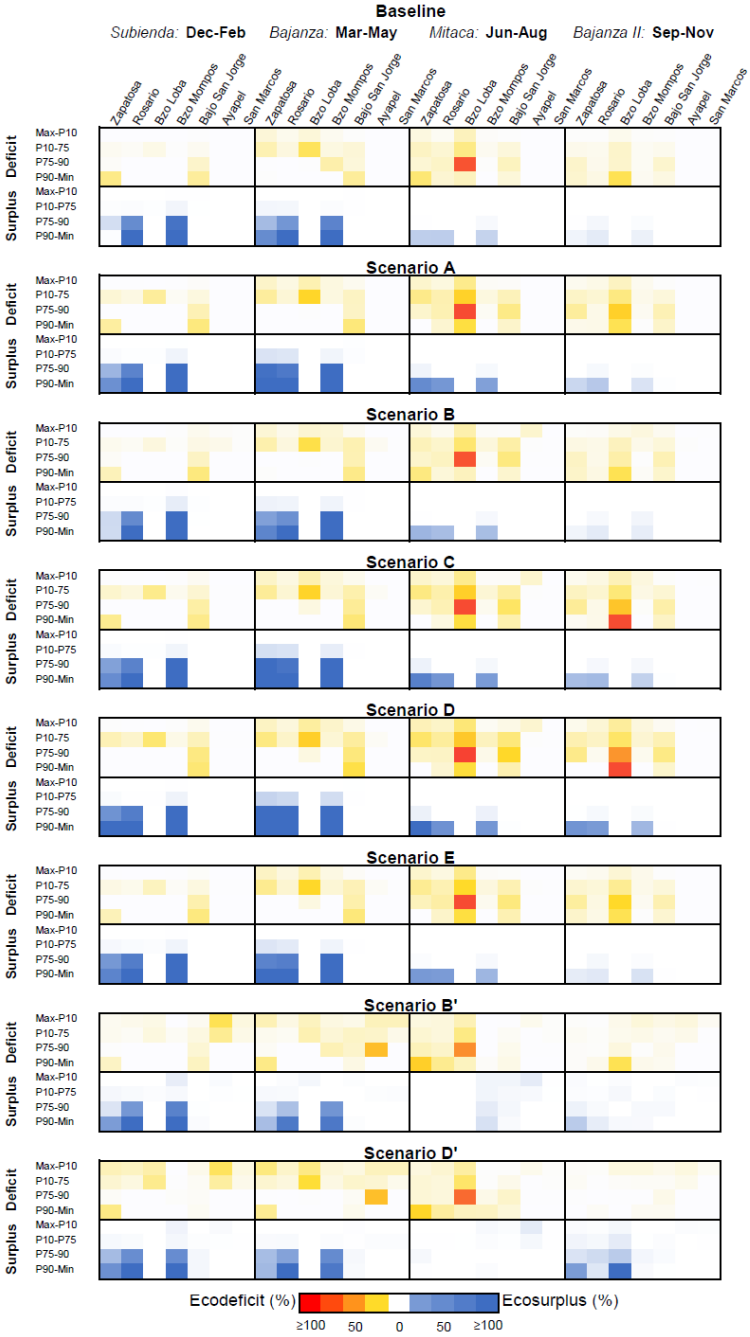

Figure 12. Impacts of upstream regulation scenarios in wetland dynamics for the different floodplain sub-units (See locations in Figure 5), expressed as Ecodeficits or Ecosurpluses in the hydroperiod. Seasons correspond to periods of biologic and hydrologic relevance, particularly to fish migration: *Subienda* (Dec-Feb), *Bajanza I* (Mar-May), *Mitaca* (Jun-Aug), and *Bajanza II* (Sep-Nov). Ranges of durations representing extreme high (*Max* to *P10*), seasonal (*P10* to *P75*), low (*P75* to *P90*), and extreme low events (*P90* to *Min*) are representative of events associated with different ecological or physical processes. Scenarios B' and D' consider an alternative operational regime of configurations B and D, to reduce flood peak magnitudes by maintaining low storage in reservoirs to allow regulation of peak flows.

Table 1. Existing and proposed hydropower projects and other related infrastructure in the MRB, used to identify dam sets.

Project name	ID	Generation capacity (MW)	Gross volume estimate (million m^3)	Dam height (m)	Median discharge (m^3/s)
Existing					
Amoyá*	42	80	*	5	21.2
Ayurá (Transfer)	134	19	*		0.6
Betania	5	540	1488.0	58	388.4
Cadena1_Casalaco*	36	261	*		
Cadena2_Pagua*	212	580	*		
Calderas	17	26	0.0	25	7.6
Canoas*	74	50	*	0	117.5
Carlos Lleras*	56	78.2	*	5	68.3
Cucuana*	36	55	*	5	5.9
El Colegio*	77	300	*		119.4
Florida 2*	121	24	*		44.3
Ituango	21	2400	1850.0	197	1133.5
Jaguas–San Lorenzo	9	170	185.0	63	55.3
Laguneta*	76	80	*	0	117.7
Miel	3	396	591.0	188	118.9
Miraflores	14	0	99.0	0	4.7
Muña	1	270	0.8	13	1.2
Neusa	60	0	101.0	0	1.6
Palmas	147	12	N/A	10	
Penol-Guatapé	6	560	1071.0	36	112.2
Piedras Blancas	135	11	2.9	0	0.8
Playas	13	201	76.8	46	128.2
Porce_2	29	426	142.7	118	172.5
Porce_3	4	660	170.0	151	201.9
Prado	12	55	1034.0	92	113.8
Quimbo	26	400	3205.0	151	228.8
Río Grande 1	7	19.9	0.5	0	99.5
Río Grande 2	8	0	153.0	65	0.1
Rio Negro	78	10	13.4	14	139.3
Salto I-II *	75	120	*		117.5
Salvajina	2	285	865.0	148	201.8
San Carlos–Punchiná	10	1020	72.0	70	145.1
San Francisco	11	135	2.3	8	0.0
San Miguel	41	44	0.3	5	102.5
San Rafael (Supply storage)	61	0	71.0	59.6	1.0
Sisga	62	0	101.2	0	2.8
Sogamoso	20	820	4800.0	190	504.0
Tafetanes *	16	0	*	0	2.3
Tasajera *	213	306	*	0	39.8
Tominé (Multipurpose storage)	63	0	690.0	30	6.9
TR Guarinó (Transfer)*	39	0	*	5	63.4
TR Manso (Transfer)*	40	0	*	5	12.0
Troneras	15	42	31.0	48	40.2

Project name	ID	Generation capacity (MW)	Gross volume estimate (million m^3)	Dam height (m)	Median discharge (m^3/s)
Proposed					
Aguadas	128	124	6.9	27	67.0
Alto Saldaña	141	124	423.2	155	97.0
Ambalema	158	208	154.4	19	1340.0
Apaví	132	1920	2639.3	120	1229.1
Aranzazu	66	102	252.6	120	119.4
Atá	142	109	197.1	135	46.0
Basilio	139	253	12680.7	112	204.2
Basillas	155	126	251.0	27	575.0
Bateas	154	145	67.4	31	520.0
Bellavista	140	197	156.6	57	109.3
Boquerón	73	104	0.6	22	30.0
Buenos Aires	69	106	1402.1	140	110.9
Butantán	79	268	1999.6	170	131.7
Cabrera	31	605	1510.1	177	327.4
Cambao	53	189	46.0	10	1260.6
Cañafisto	22	965	6487.8	139	1039.2
Cañaveral	34	80	1.0	32	19.1
Carare	117	582	1408.8	22	2287.4
Carbonero	115	269	217.4	14	2085.2
Carolina	116	349	213.1	16	2123.3
Carrasposo	156	150	151.0	27	675.0
Cepitá	103	172	19.7	25	192.0
Chacipay	86	164	310.2	85	167.1
Chagualo	137	100	188.1	97	116.5
Chillurco	149	161	359.1	105	126.0
Chimurro	120	146	N/A	0	27.3
Cocorná	97	33	7.0	42	22.3
Coyaima	145	110	360.8	34	246.0
Cuerquia	130	75	8.8	57	5.1
El Indio	90	107	245.6	70	125.9
El Juncal	107	115	202.1	27	421.3
El Manso	152	118	163.8	29	425.0
El Neme	143	480	5670.0	185	182.0
El Palmar	131	91	0.2	20	7.7
El Tablón	102	171	6.2	25	144.2
Encimadas	33	94	2.7	35	10.5
Escuela_Minas	38	55	0.1	5	66.2
Espíritu Santo	18	885	185.3	81	1167.5
Farallones	127	2120	11916.9	220	802.2
Filo Cristal	105	262	125.1	36	527.0
Fonce	100	343	77.7	65	113.0
Furatena	85	125	2989.9	115	122.6
Guaira	93	115	357.8	66	43.8
Guane	104	426	1063.5	160	337.5
Guarapo	148	104	533.4	100	106.0
Guarquina	94	69	60.5	71	68.8
Hispania	129	145	3.6	27	43.3
Honda	159	374	663.3	31	1370.0
Horta	88	114	1463.2	150	101.3
Icononzo	72	117	0.2	20	25.6
Isnos	64	103	33.3	105	16.3
Julumito	122	53	165.1	80	55.0

Project name	ID	Generation capacity (MW)	Gross volume estimate (million m^3)	Dam height (m)	Median discharge (m^3/s)
La Cascada	70	70	0.3	18	12.5
La Chamba	110	169	231.3	19	981.4
La Dorada	112	323	229.6	21	1385.3
La Miel II	35	120	0.5	5	41.1
La Plata	68	159	225.6	120	60.2
La Playa	71	84	2.9	25	22.0
La Suecia	82	66	38.0	100	14.7
La Vieja	124	80	1246.2	90	151.5
Lagunilla	83	60	0.3	15	30.9
Lame	157	334	236.6	28	1270.0
Lebrija	106	187	3269.4	145	108.4
Mamaruco	98	167	678.4	135	185.2
Marañal	113	461	612.1	26	1555.7
Mayaba	32	242	230.2	50	455.3
Nariño	50	356	118.0	20	1161.8
Natagaima	108	154	231.1	26	606.2
Nus	91	189	12.7	95	99.5
Ombale	146	105	98.0	34	238.0
Oporapa	150	180	699.7	130	130.0
Páez	67	143	81.8	90	54.2
Paicol	65	311	1570.6	170	184.2
Palmalarga	144	496	7737.3	160	296.0
Palmera	95	312	838.8	106	135.1
Patagón	114	170	102.2	12	1729.4
Pericongo	151	240	1245.6	120	136.0
Piedra del Sol	30	420	257.1	125	127.4
Piedras Negras	55	299	13.7	15	1343.1
Porce 4	19	404	2198.1	195	223.4
Porvenir 1	24	364	1384.9	167	166.6
Porvenir 2	23	352	463.0	145	186.2
Puente Linda	80	52	88.9	90	55.1
Riachón	136	100	1.4	50	10.9
Ricaurte	111	141	90.8	16	1043.0
Risaralda	125	93	25.8	60	23.0
Samal	84	107	623.0	140	53.4
Samaná Medio	25	175	1668.8	177	130.3
San Diego	81	54	109.9	87	8.9
San Juan	37	114.3	0.2	5	64.6
Santo Domingo	96	48	3.1	23	35.5
Simacota	99	162	140.3	90	245.0
Socotá	101	124	1.6	22	109.2
Tamar	92	132	642.6	60	111.1
Timba	123	60	782.4	46	254.2
Toloso	133	334	167.7	26	1309.1
Troya	89	151	2341.2	150	123.8
Valdivia	138	700	728.9	128	140.6
Veraguas	153	110	202.3	26	490.0
Vigía	109	132	80.4	20	618.4
Wilches	119	308	34.8	11	3269.1
Xarrapa	126	330	351.0	66	776.7
Yátaro	87	150	1589.9	90	144.4
Yondó	118	308	129.3	12	2684.4

Note: Main projects are labeled with ID in Figure 1. *: Run of river projects

Table 2. Indices of basin-level cumulative alteration of selected scenarios at Mompós Depression boundary conditions. See Figure 5 for station locations.

Scenario	Installed capacity (MW)	Weighted degree of regulation (%)			Connected main river network km and (%) loss		Cumulative sediment trapping (%)		
		Magdalena	Cauca	Nechí	0 to 400 masl	400 to 1000 masl	Magdalena	Cauca	Nechí
Baseline	9781	5.2	4.8	0.6	6789 (2.5)	1104 (54)	40.9	79.2	24.6
A	14856	8.5	4.9	2.9	6763 (2.9)	1021 (57.5)	47.2	79.3	27.1
B	15603	6.2	39.1	4.3	6637 (4.7)	975 (59.4)	40.3	66.7	66.7
C	15081	15.3	19.0	2.1	6433 (7.6)	485 (79.8)	60.7	67.9	52.6
D	15635	23.5	19.3	24.5	4791 (31.2)	143 (94.1)	80	78.7	66.2
E	14771	13.2	5.7	2.9	6703 (3.7)	937 (61)	58	66.6	50.7

SI-1. SUPPLEMENTARY INFORMATION

ReservoirSimulator model description

The ReservoirSimulator allows simulation of the water balance of a group of reservoirs, based on individual or system-level dispatch rules for three main categories of use: downstream instream requirements, hydropower, and other supply (supply that bypasses turbines).

For a given reservoir, the model takes into account physical and technical constraints, such as the volume-elevation curve, tail-water elevation, operational levels (inactive, buffer, technical, and safety), turbine type, capacity, and efficiency. It allows modeling of the topology of reservoirs and tributary sub-basins.

ReservoirSimulator performs a lumped, discrete-time water balance of the components shown in Figure SI-1 with the model parameters and inputs shown in Table SI-1.

For each reservoir, calculations are done according to the sequence in Table SI- 2:

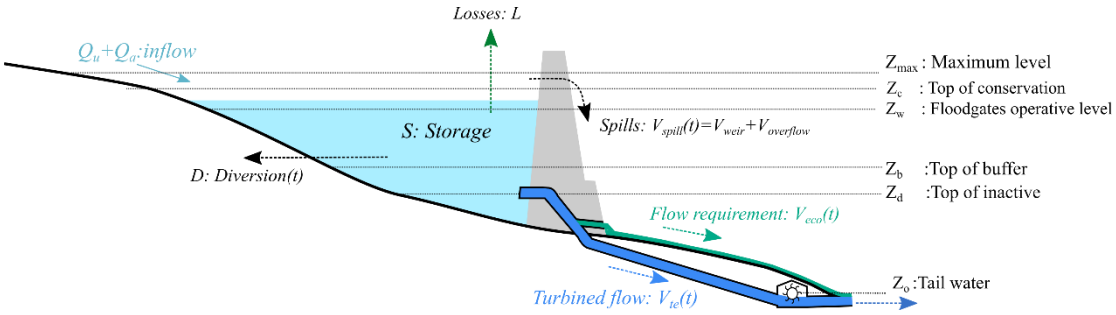

Figure SI- 1: Schematic of reservoir inflow, outflow and storage components of the reservoir simulator model.

Table SI-1: Description of reservoir data requirements of the model

Symbol	Reservoir physical and technical data	Units
$Q_a(t)$	Specific runoff: Runoff from upstream sub-watershed during step *t* (excludes outflows from upstream infrastructure)	m^3/s
Δt	Time step	s
V_c	Reservoir storage capacity at top of conservation level (Z_c)	m^3
V_{buffer}	Reservoir storage capacity at buffer level (Z_b)	m^3
V_{min}	Reservoir storage capacity at top of inactive level (Z_d)	m^3
V_{w0}	Reservoir storage capacity at floodgates operative level (Z_w)	
H(V)	Volume-elevation curve of reservoir	masl
A(V)	Area-elevation curve of reservoir	masl
B_c	Buffer coefficient: fraction of buffer storage that can be allocated in a given time step *Note: Can be a user defined function of local (i.e. reservoir storage, etc.) or system-level state variables or context variables (i.e. downstream storage, etc.).*	%
B_w	Floodgates allocation factor: determines the fraction of storage above the floodgates operational level delivered downstream in a given time step. *Note: Can be a user defined function of local (i.e. reservoir storage, etc) or system-level state variables or context variables (i.e. downstream storage, etc.).*	
ET(t)	Evaporation rate in a time step *t*	mm
Z_0	Tail water elevation (water level at the point where turbine flow is discharged)	masl
D(t)	Water demand diverted from the reservoir, bypassing the turbines, with higher priority than hydropower	m^3
$V_{eco,1}(t)$	Average instream flow requirement at step *t*, for the reach between reservoir and turbines discharge	m^3
P	Installed generation capacity	Mw
f	Friction loss factor in hydropower load pipes.	m
N	Number of turbines	
E(H,Q)	Turbine efficiency curve, as a function of net head and flow (typically a function of turbine type i.e. Francis, Pelton, etc.)	%
e_{target}	Minimum efficiency threshold of turbines. Hydropower won't be generated if actual efficiency is lower than e_{target}	%
Q_w	Floodgates max hydraulic capacity	m^3/s
Reservoir topological data		
K_T	Identifier of the project downstream of turbine flow discharge	
K_E	Identifier of the project downstream of e-flow discharge	
K_s	Identifier of the project downstream of spills discharge	
R	Position of the reservoir in the simulation sequence (1st, 2nd, …)	

Table SI- 2: Sequence of calculations performed by the reservoir simulator model at a given time-step

Value	Description	Calculation	Units
$Q_u(t)$	Sum of upstream outflows (turbine, e-flows and/or spills) directed to the reservoir		$[m^3/s]$
S_t	Reservoir storage at the beginning of step t		$[m^3]$
A_t	Area of reservoir at the beginning of step t, calculated from area volume curve	$A(S_t)$	$[m^2]$
L	Reservoir losses as evaporation	$A_t * ET$	$[m^3]$
Va_t	Total available water for allocation without restrictions at the reservoir, during step t	$\max(0, S_t + (Q_a(t) + Q_u(t)) * \Delta t - L(t) - V_{buffer})$	$[m^3]$
Vr_t	Total available water for allocation, from the buffer zone, during step t	$(V_{buffer} - V_{min}) * B_c$: if $Va_t > 0$ $(S_t + Q_a(t) * \Delta t - L(t) - V_{min}) * B_c$: if $Va_t = 0$	
Vu_t	Total available water for allocation during step t	$Vr_t + Va_t$	
Z_t	Reservoir water level at the beginning of step t, calculated from volume elevation curve	$Z(S_t)$	masl
ΔZ_t	Working water head at step t.	$Z_t - Z_0$	[m]
H_f	Friction losses	$\Delta Z_t * f$	[m]
RPE	Expected generation at step t, expressed as a percentage of installed capacity.	User defined function of local (i.e. reservoir storage at previous timestep, instream flow requirement downstream of turbines, etc) or system-level state variables or context variables (i.e. system level demand, ENSO signal, etc.). See paper Figure 3	[%]
V_{pt}	Release requirement, to fulfill 100% of expected energy generation at step t, operating at target efficiency	$RPE * P * 1e6 / (9801 * (\Delta Z_t - H_f) * e_{target}) * \Delta t$	$[m^3]$
Vd_t	Total water available during step t, after the allocation of demands with higher priorities than hydropower	$\max(0, Vu_t - D_t - V_{eco,1})$	$[m^3]$
V_{te}	Effective turbined volume during step t	$\min(V_{pt}, Vd_t t)$	$[m^3]$
Q_{te}	Effective turbined flow during step t	$V_{te}/\Delta t$	$[m^3/s]$
Vs_t	Water available after hydropower is allocated.	$Vd_t - Vt_e$	$[m^3]$
V_w	Controlled spill volume (floodgates operation)	$V_w = \min\left(R_w^{1/B_w}, Q_w * \Delta t\right)$ with: $R_w = \max(0, Vs_t - V_{w0})$: Volume above the floodgates operational level	$[m^3]$
Vs_w	Water available after controlled spill is allocated.	$Vs_t - V_w$	$[m^3]$
V_{spill_t}	Total spill during step t	$\max(0, Vs_w - Vc)$	$[m^3]$
P_n	Net power output if available flow is turbined given $H_{n,t}$, using n turbines.	$\gamma * \frac{Q_{te}}{n} * H_{n,t} * e_{t,n}$	[Mw]
$e_{t,n}$	Actual Turbine/Generator efficiency given $(\Delta Z_t - H_f)$ and flow = $\frac{Q_{te}}{n}$. See example in	e_n 0 if $e_n < e_{target}$	%

Value	Description	Calculation	Units
	Figure SI-2. If efficiency is lower than a target efficiency, is adopted as 0.		
P_t	Actual power output for step t	$\max(P_1, 2 * P_2, \dots N * P_N)$	[Mw]
S_{t+1}	Reservoir storage at the beginning of step t	$Vs_t - V_{spill_t}$	m^3

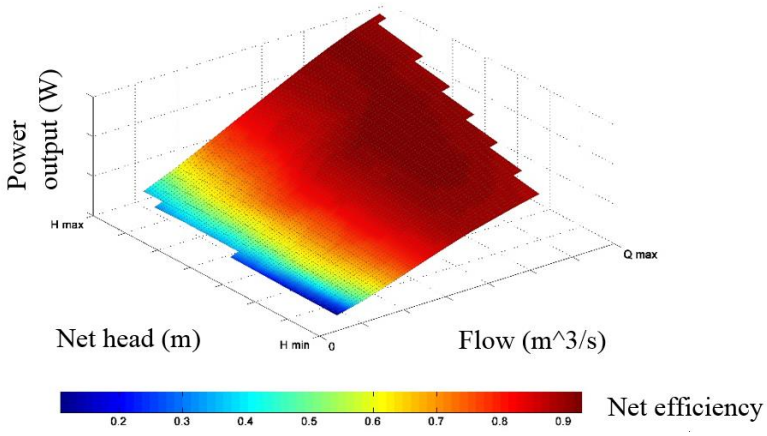

Figure SI-2 Example of a turbine power-efficiency function (Francis type)